RECONSTRUCTING THE DEVILS CASTLE ROCK AVALANCHE, ALBION BASIN, UTAH

by

Patricia Pedersen

A thesis submitted to the faculty of
The University of Utah
in partial fulfillment of the requirements for the degree of

Master of Science

in

Geological Engineering

Department of Geology and Geophysics

The University of Utah

May 2018

The University of Utah Graduate School

STATEMENT OF THESIS APPROVAL

The thesis of **Patricia Pedersen**

has been approved by the following supervisory committee members:

Jeffrey Moore	, Chair	**January 19, 2018** Date Approved
Michael Thorne	, Member	**January 19, 2018** Date Approved
Richard Giraud	, Member	**January 19, 2018** Date Approved

and by **Thure Cerling**, Chair/Dean of

the Department/College/School of **Geology and Geophysics**

and by David B. Kieda, Dean of The Graduate School.

ABSTRACT

Rock avalanches are high-magnitude, low-frequency mass wasting events characterized by high mobility and fluid-like runout motion. Yet, little information is typically available to describe the hazard posed by these events because of their scarcity. Geologic records thus provide key data regarding rock avalanche metrics, such as size, timing, and dynamics needed to characterize the hazard. In this study, we present a detailed case history analysis of the Devils Castle rock avalanche located near the town of Alta in the Wasatch Mountains of Utah. The deposit is approximately 1.5 km in length with a Fahrboeschung angle of 14°. Through topographic reconstruction, we calculate a deposit volume of 1.7 million m^3, with a maximum thickness of 25 m and an average thickness of 7 m. We estimate a bracketed age of occurrence as 11,000 to 16,000 years old from limiting radiometric and cosmogenic exposure ages. The Devils Castle headwall is complex with no obvious evidence to indicate the precise source location and geometry. Therefore, we reconstructed two plausible source areas and ran 3D numerical runout simulations for each. Results agree well with mapped deposit boundaries for both source scenarios. However, the east source model

better represents material and dynamic characteristics of the deposit (e.g., lithology, superelevation) observed in the field. The rock avalanche is located near the seismically active Wasatch fault zone, and we identified five additional, similar events in the region highlighting the extent of the potential hazard. Individual case history analyses such as this allow us to better understand the processes and controls of similar large-scale mass movements, and ultimately evaluate the risk posed by these extreme events.

Civilization exists by geological consent,
subject to change without notice.

Will Durant

TABLE OF CONTENTS

LIST OF FIGURES

Figures

LIST OF TABLES

Tables

ACKNOWLEDGMENTS

First, thank you to my committee members Mike Thorne, who teaches a most interesting geophysics class and who took this committee assignment on despite his expertise lying elsewhere, and Rich Giraud who initially introduced this study to my advisor and has been a valuable resource of knowledge of the area. From my undergraduate days, a quick thanks goes to my favorite field partner, Parker, and David the TA. Without them, I might not have made it through field camp. Remember to keep Mama Trish happy. I would be remiss if I did not give my appreciation to my advisor, Jeff Moore. His help through this process has been invaluable. He guided me through research during my undergraduate degree and directed me through the last bit of my master's degree. From the beginning of our time together, when I demanded a project from him, to now, he has been a solid support for me to lean on. Finally, to the man who has been through it all with me, Tristan, thank you. Your patience in the field while my ankle was recovering and your openness to my geological musings are memories I will always cherish and carry in my heart. Thank you for your unwavering support, your love, and for helping make my lifelong dream of becoming a geologist a reality.

INTRODUCTION

With rapid and flow like runout, rock avalanches represent a high-magnitude landslide hazard (Aaron and Hungr, 2016). These mass wasting events tend to be rare but can be highly destructive, making an understanding of their mechanics crucial in areas where the potential for destruction of property or loss of life is large (Christenson and Ashland, 2006; Willenberg et al., 2009; Loew, 2012). Generating and compiling geologic records from prehistoric rock avalanche case histories provide key data necessary for modern hazard and risk assessment; these include essential hazard parameters such as volume, age, and failure dynamics.

Understanding landslide mechanics is critical for characterizing landslide hazard. Rock avalanche runout behavior depends on the source and runout path materials and substrate, topography, and additional effects such as entrainment of water (Hungr and Evans, 2004; Dufresne, 2009). Compiling geologic case history data allows us to characterize rock avalanche hazards regionally and globally, which may be especially critical in areas with long recurrence intervals and no historical data. Calibrated case histories, in turn, allow us to generate numerical runout models that can be

used to predict rock avalanche reach and impact velocities, and quantitatively assess risks stemming from similar event scenarios (Hungr and Evans, 1996; Hungr and McDougall, 2009; Aaron and Hungr, 2016). Further key for evaluating rock avalanche hazards is determining the absolute age of events and, in turn, recurrence intervals. Whereas in the past, radiocarbon dating was often used to provide limiting ages for large landslides (McCoy, 1977; Madsen and Currey, 1979), today cosmogenic nuclide surface exposure dating is the predominant tool used to establish absolute timing information (Ballantyne et al., 1998; Ivy-Ochs and Kober, 2008; Grämiger et al., 2016).

Large rock slope failures originating from near-vertical cliffs are also an important mechanism contributing to the morphological development of glacial landscapes (Stock and Urhammer, 2010). Glacial erosion undercuts cirque headwalls (Sanders et al., 2012), and although the efficacy of glacial debuttressing has been called into question (McColl et al., 2010; McColl, 2012), rock debuttressing through undercutting is an important factor generating rock mass damage and conditioning future slope failures (Grämiger et al., 2017). Triggering factors for rock avalanches typically include seismicity and heavy precipitation or snowmelt (Stock and Urhammer, 2010; Coe et al., 2016), although many historical events have occurred without any recognizable trigger (Lipovsky et al, 2008; Coe et al., 2017).

Earthquake hazard scenarios have been developed for the Wasatch Fault due to the large population that resides in the seismically active region (Pankow et al., 2015). The Wasatch Front, which is a part of the Intermountain Seismic Belt, has a long history of seismic activity (Swan et al., 1980; DuRoss, 2008). Detailed past studies from several paleoseismic trench sites along the Salt Lake City segment of the Wasatch Fault reveal an average recurrence interval of ~1350 years for surface-rupturing earthquakes (McCalpin, 2002; DuRoss, 2008). Meanwhile, several other rock avalanches are also found along the Wasatch Front (Hooper, 1951; Cardoso, 2002; Ashland and McDonald, 2008). Study of these slides may be of critical importance for seismic hazard scenarios if these are thought to be predominantly coseismic.

Here we study the Devils Castle rock avalanche located in the Albion Basin near the town of Alta, Utah. We begin by describing the rock avalanche extents, deposit lithology, and surrounding Quaternary landforms. We then reconstruct the preslide topography to generate a rigorous estimate of the deposit volume, and project that material onto the headwall in two likely source areas. We use these topographic reconstructions as the basis for 3D runout modeling, which provides key insights on the landslide mobility and dynamics of the failure. Finally, we compile key data from other similar rock avalanche events found in and around the Wasatch Front in order to highlight the frequency and potential impacts of these large landslides.

STUDY AREA

General Background

The Devils Castle rock avalanche is located at the head of Little Cottonwood Canyon, in the Wasatch Mountains near Salt Lake City, Utah, USA. The area is an alpine basin with a floor at approximately 2800 m and the summit of Devils Castle reaching an elevation of 3400 m above sea level. The rock avalanche released from the headwall of Devils Castle as a slab, fragmented, and cascaded into a north trending low relief strike gully formed between two east dipping quartzite ridges.

The Albion Basin is south of the Town of Alta, Utah, which was founded as a mining town in 1871 (Robertson, 1972). Mining in the area peaked in the 1880s and declined with one major boom in the 1900s (Robertson, 1972). During the 1930s, Alta transitioned from mining to recreational skiing (Shrontz, 1989). Since then, the Albion Basin has become a highly utilized recreation center in close proximity to the Salt Lake Valley. With a network of trails, visitation in the summer can be upwards of 10,000 people per week (David Evans and Associates, 2011), with the most heavily accessed trail passing directly through the rock avalanche deposit. The ski

area maintains multiple runs below Devils Castle, and a restaurant directly at the toe of the rock avalanche deposit.

Geologic History

Bedrock geology of the Albion Basin consists of sedimentary and metamorphic rocks ranging in age from Pre-Cambrian to Mississippian, with an Eocene intrusion cutting the layers. The oldest unit is a tillite developed when glaciers advanced over modern day Utah from metamorphic highlands to the edge of the Panthalassan Ocean (Case et al., 2005). As the glaciers retreated, the ocean underwent a transgressive sequence creating beds of Tintic Quartzite, Ophir Shale, and Maxfield Limestone.

An unconformity spanning 145 million years occurs between the Maxfield Limestone and the sequence of Mississippian rocks in our study area consisting of the Fitchville Formation, and the Deseret and Gardison Limestones, being deposited in vast, inland seas. After the sea departed, the study area was subject to 150 million years of deposition and subsequent erosion, and during this time, the Sevier Orogeny created the thrust faults seen through the area (Allmendinger, 1992). Later, numerous igneous intrusions occurred along the Wasatch Front, including the Alta stock dated at 33 million years old (Crittenden, 1976), which were cut by normal faults occurring after the Sevier Orogeny (Baker et al., 1966). Around 17 million years ago, the basin and range province was at its infancy and the Wasatch

Fault was created (Crittenden, 1976). During this time, the Salt Lake Valley broke away from the mountains along a normal fault, with the valley down-dropping and the mountains uplifting (Crittenden, 1976). Finally, throughout the Pleistocene, the area was subject to several glaciations, creating the large mountain cirque of the Albion Basin.

The geomorphology of the area consists of glacially and periglacially modified landscapes (Figure 1). Above the rock avalanche deposit, there are several (possibly active) rock glaciers and a large talus pile originating from the western part of the headwall, as well as a large talus cone with its apex at the eastern part of the headwall. Glacial and periglacial deposits modified, reorganized, and cover the uppermost portion of the rock avalanche deposit. The rock avalanche has blocked some of the natural drainages creating bogs within and around the deposit, the largest of which is located in a meadow directly above the toe.

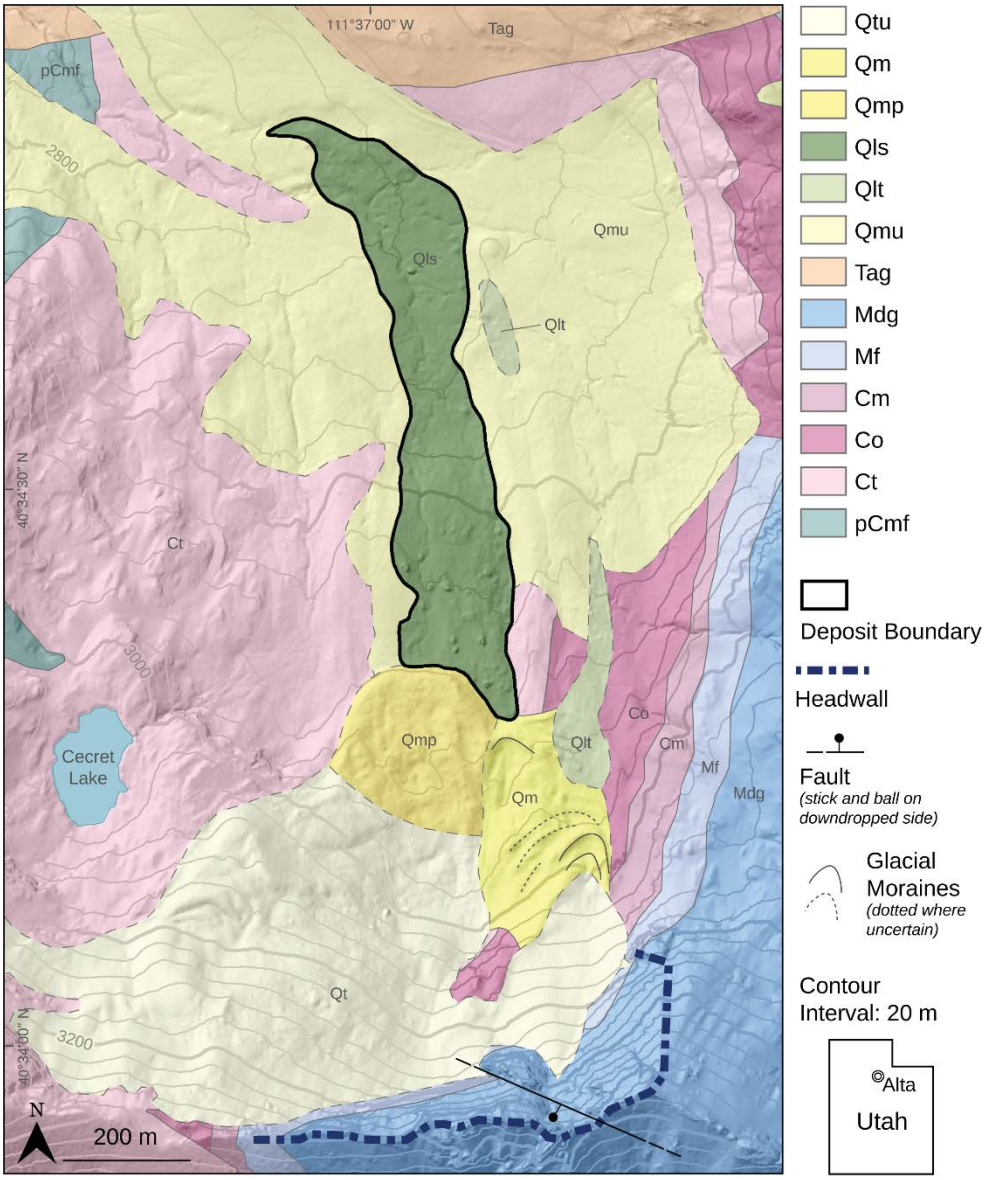

Figure 1
Geologic map of Albion Basin (adapted from Baker et al, 1966). Bedrock and some glacial units adapted, other surficial units mapped by author. The rock avalanche originated from Mississippian limestone and partially covered existing glacial deposits. Later glacial and periglacial deposits covered the upper portion of the slide. Note the thin lateral deposits to the east of the main body. Rock units include: Undifferentiated talus (Qtu), Glacial deposit (Qm), Periglacial deposit (Qmp), Landslide deposit (Qls), Landslide deposit, thin layer (Qlt), Glacial deposit, undifferentiated till (Qmu), Alta Stock (Tag), Deseret and Gardison Limestone, undivided (Mdg), Fitchville Formation (Mf), Maxfield Limestone (Cm), Ophir Formation (Co), Tintic Quartzite (Ct), Mineral Fork Tillite (pCmf).

DEVILS CASTLE ROCK AVALANCHE

Deposit Description

We generated a detailed geologic map providing a description of key deposit characteristics including lithology, boundaries, runout, thickness, and superelevation (Figure 1). We also noted possible source areas for the rock avalanche. We utilized available resources including aerial photography, previously published geological maps (Baker et al., 1966), and a LiDAR (Light Detecting and Ranging) digital elevation model (Utah Automated Geographic Reference Center. 2006) to aid field mapping. Important Quaternary erosional and depositional features observed in the field neighboring the rock avalanche deposit were also incorporated.

The deposit consists mainly of Mississippian Deseret/Gardison limestone boulders with some Fitchville limestone boulders, and the boulders can measure up to 6 m in height. The limestone is a dark grey fossiliferous biomicrite with quartz veins and chert nodules throughout (Baker et al., 1966). The blocks are typically weathered, often appearing broken and crumbled (Figure 2d). Very large boulders tend to be located toward the boundaries of the slide. The deposit and its perimeter were easily identified

in most places during field inspection. However, toward the top of the deposit, rock avalanche debris has been modified, reorganized and covered by glacial and periglacial deposits, while the toe has been modified by construction of a restaurant.

Features of the rock avalanche deposit are strongly controlled by topography. Erosion resistant bedrock outcrops throughout the basin create parallel strike-gullies. The deposit is located within one such gully. The observable length of the rock avalanche deposit is approximately 1 km (Figure 2a). From geological reconstruction, we estimate the original length of the rock avalanche deposit to be approximately 1.5 km. The slide is at maximum 195 m wide at the top, and narrows to 80 m wide (Figure 2a) where the gully narrows.

The distal and proximal ends of the deposit consist of several notable features. Periglacial and glacial landforms cover the top of the deposit with the upper most glacial deposits consisting of a set of nested moraines approximately 135 m across (Figure 1). Smaller moraines are found through the section under Devils Castle. Periglacial deposits consist of rock glaciers, the largest being an apparently inactive feature approximately 250 m across (Figure 1). At the toe of the deposit, large boulders of the rock avalanche deposit are observed, but abruptly end right before the restaurant. We did not observe any other signs of the deposit further down the drainage from the restaurant in field observations, and using 1940 and 1963 aerial photography

(Utah Geological Survey Aerial Imagery Collection) we did not see anything more as well.

Along the east side of the main deposit, a smaller collection of boulders was identified, which we estimate averages at most 2 m thick (unit Qlt, Figure 1), extending to the base of the nested moraines. In this area, large boulders cover and comingle with glacial deposits (unit Qmu, Figure 1) consisting of low-amplitude moraines and till. This thin deposit follows a gully that parallels the main slide for up to 500 m through an area presently occupied by cabins and ends above the Albion Basin campground. One other smaller thin deposit (unit Qlt, Figure 1) is found east of the narrowest neck of the rock avalanche deposit (Figure 1). This area consists of a few large boulders on the surface, and due to construction of a ski lift, the subsurface has been exposed showing boulders as large as 1 m across.

The rock avalanche deposit has created several bogs by impeding and rerouting the natural drainage system. The most extensive of these is found just above the toe of the rock avalanche deposit in a large meadow area approximately 300 m in length. Another bog of interest is located on the lower eastern side of the deposit just outside the boundaries and parallels the large meadow bog. This bog is created by a different stream that cuts around the east of the deposit and is impeded by the rocks of the deposit. In other parts of the deposit, the bogs are smaller and tend to have interspersed boulders.

Age

Determining the age of the rock avalanche deposit allows us to comment on potential triggers for the event, such as known paleoseismic earthquakes, if any exist, and allows us to place the event in geological context to discuss preparatory influences of glacial history and climate change. Previously reported radiocarbon dates provide a minimum limiting age for the Devils Castle rock avalanche: Madsen and Currey (1979) found a ^{14}C age of 8162 to 8484 cal BP (recalculated calibrated 1σ range using IntCal13; Reimer et al., 2013) for humic colluvium sampled from inside the nested moraines (sample GX-4644), and 10,571 to 11,205 cal BP (sample RL-695) and 10,397 to 11,103 cal BP (sample GX-4736) from wood and peat at the base of a bog overlying the rock avalanche deposit (McCoy, 1977).

We used cosmogenic nuclide surface exposure dating to determine the age of the Devils Castle rock avalanche. Cosmogenic nuclides are created in constituent rock surfaces through exposure to cosmic rays (Anderson and Anderson, 2010). The concentration of these nuclides is an indicator of the length of time a rock surface has been exposed, assuming the sampled surface was initially inside the cliff under more than a few meters of rock, and that the test surface has not eroded significantly or been reburied since original exposure (Ballantyne et al., 1998; Ivy-Ochs and Kober, 2008). When determining the production rate of nuclides, we take into consideration the depth to which cosmic rays travel into the material, and its density

(Anderson and Anderson, 2010). In our case, we use cosmogenic ^{36}Cl dating, which is the preferred nuclide for limestone because of the high calcium content found in a carbonate rock, a target for production of ^{36}Cl (Ivy-Ochs et al., 2009).

Boulders selected for dating were chosen following Ivy-Ochs and Kober (2008); we selected relatively large boulders with a flat top surface with weathered 'old' appearance and minimal flaking. We chose six boulders in total along the length of the deposit. Samples from the boulder surfaces were collected using a portable tile saw, hammer and chisel, where an approximately 20 cm square was chipped out to a depth of 2–3 cm. The samples were then crushed and sieved and sent to the PRIME lab at Purdue University to measure the concentration of ^{36}Cl. Final cosmogenic age results are pending.

Volume and Runout

In order to quantify the volume of the Devils Castle rock avalanche, we carefully reconstructed a probable prefailure basal topography using a 10 m grid resolution. We interpreted the subsurface by extrapolating existing surface features, such as the slope of current topography, to a reasonable prefailure surface structure. Internal consistency was maintained through comparison of key features, depth for example, between each profile. The outcome of this process was 42 cross profiles and 1 longitudinal profile across

the deposit (see Appendix). These results allowed us to quantify the thickness and volume of the rock avalanche, and additionally to use numerical runout modeling to explore the dynamics of failure. After creating the profiles, we digitized and regridded the basal surface data generating a plausible prefailure topography. Differencing the recreated topography from the current topography, we determined the rock avalanche volume as 1.7 x 10^6 m^3, which is presumed accurate within ±25% through analysis of error (see following Discussion). Topographic reconstruction further allowed us to estimate the spatial distribution of thickness of the rock avalanche deposit (Figure 3a). We found thicker deposits at the distal and proximal ends of the rock avalanche, where topography flattens, while thickness in the middle of the deposit is lower accompanying an increase in steepness of the basal long profile. The maximum thickness of the deposit is 25 m with an average thickness of 7 m.

To determine the mobility of the slide from field and topographic data, we measured the Fahrboeschung angle, or the ratio of the fall height to path length connecting the highest point of the source and most distal point of the deposit (McDougall et al., 2012). This value was found to be at 14° for the Devils Castle rock avalanche (H/L = 0.25).

Two points of deposit superelevation were identified from field observations (Figure 2a) and found during the reconstruction process (Figure 4). The first occurs one-third of the way down the deposit where the surface

is superelevated approximately 10 m rising to the west (Figure 4a). The second occurs at the lowermost bend just before the toe of the deposit, where the surface is superelevated approximately 10 m to the east (Figure 4b). Minimum rock avalanche velocity needed to attain the measured superelevation can be estimated as (Jibson et al., 2006):

$$V_{min} = \sqrt{\frac{ghr}{w}} \qquad \text{(Eq. 1)}$$

where V_{min} is the minimum velocity (neglects basal resistance), g is gravity, h is the superelevation height of the deposit at the bend, r is the radius of the bend, and w is the width of the channel. Using Eq. 1, we determined the minimum speed of the rock avalanche was ~27 m/s at the upper point and ~15 m/s at the lower point.

Source Area

The source headwall of the Devils Castle rock avalanche exhibits a near vertical face in some areas and is almost 1 km across (Figure 2b). The headwall consists of the Deseret/Gardison limestone, as found in the deposit. However, a well-defined evacuated source area for the rock avalanche is not apparent. Inspecting for possible source areas on the complex topography of the headwall, we identified two possibilities: an east and west source that

could match field observations. As a result, we independently created and analyzed two source areas for runout modeling purposes. The first contains an evacuated area and a west facing wall toward the eastern side of the headwall (east source), while the second consists of a long, north facing cliff toward the western side of the headwall (west source). We modeled the reconstructed cliff after the existing headwall by extending the cliff face out and raising the peaks and ridges slightly. Then we recreated the topography of each possible source by applying the same method used in recreating the basal topography, with the unbulked deposit volume as a control. The unbulked volume was used because it is the initial volume of rock that collapsed from the cliff face, which then undergoes a fragmentation bulking process as the sliding mass disaggregates (Hungr and Evans, 2004).

Runout Modeling

Numerical runout simulation provides insight into the dynamics of rock avalanche runout behavior, additional velocity estimates, and allows us to evaluate failure scenarios involving the east and west potential source areas. We used DAN3D for runout simulation (Hungr and Evans, 1996), which is an equivalent fluid runout model with several rheologies available for basal flow resistance (Sovilla and Bartelt, 2002; McDougall and Hungr, 2004; Hungr and McDougall, 2009). We modeled the Devils Castle rock avalanche using a Voellmy rheology which provided the best match observed

deposit extents and estimated thickness. Voellmy rheology applies the following basal resistance (Hungr and McDougall, 2009):

$$\tau_{zx} = -\left(\sigma_z f + \frac{\rho g v^2}{\xi}\right) \quad \text{(Eq. 2)}$$

where τ_{zx} is the basal resistance, σ_z is the bed-normal total stress, f is the friction coefficient, ρ is the density, v is the depth-averaged velocity, and ξ is the turbulence coefficient. Both f and ξ are calibrated parameters (Hungr and Evans, 1996), which were systematically adjusted until the model result best matched our field observations.

Using the recreated paleopath topography and source area topographies for the east and west source scenarios, we modeled runout of the rock avalanche using calibrated variables from previously published studies as a starting point (Hungr and Evans, 1996; Hungr and McDougall, 2009; Aaron and Hungr, 2016). Through trial and error, we discovered that each of the two source scenarios can be modeled successfully by using the same Voellmy rheology parameters summarized in Table 1.

Models for both the east and west source areas have similar dynamics despite the different initial geometries (Figure 5); the source collapse is funneled into the main gully and continues to run out reaching generally similar extents (Figure 3b and 3c). However, there are distinct differences between the two scenarios. After collapse, the east source model spreads and

separates into three lobes, with the majority of debris traveling into the main gully (seen at 20 s into the simulation; Figure 6). One of the three lobes falls into a gully parallel to and east of the main lobe and continues down, while the other lobe proceeds into a smaller gully to the west and eventually terminates. In the west source model, the source collapses and splits into two lobes, and runs out in a similar manner as the east source, but does not include the eastern gully runout (seen at 30 s into the simulation; Figure 7). Another difference is seen at ~30 s into simulation (Figure 5c) where the east source model superelevates as it enters the main gully, while the west source model does not superelevate until 250 m above the toe of the deposit. The east source simulation with two superelevation points better matches field observations.

The simulated thickness and distribution of the deposits from DAN3D match relatively well to our thickness reconstruction from field evidence (Figure 3). Both east and west source models produce a similar thickness distribution. However, when compared to the reconstructed thickness, the models tend to place thicker deposit toward the middle area and thinner deposits toward the toe.

We determined values for maximum runout velocity and superelevation velocity estimates from DAN3D simulations of the east and west source failure scenarios. The east source failure attains a maximum velocity of ~62 m/s, and has two superelevation points closely matching those

discovered during field mapping. The upper superelevation point has a modeled velocity of 25–30 m/s, while the lower superelevation point has a modeled velocity of 10–15 m/s. The west source failure attains a maximum velocity of ~57 m/s, but has only one superelevation point toward the toe of the deposit, which has a velocity of 10–15 m/s, similar to the east source superelevation velocity at the same point near the toe.

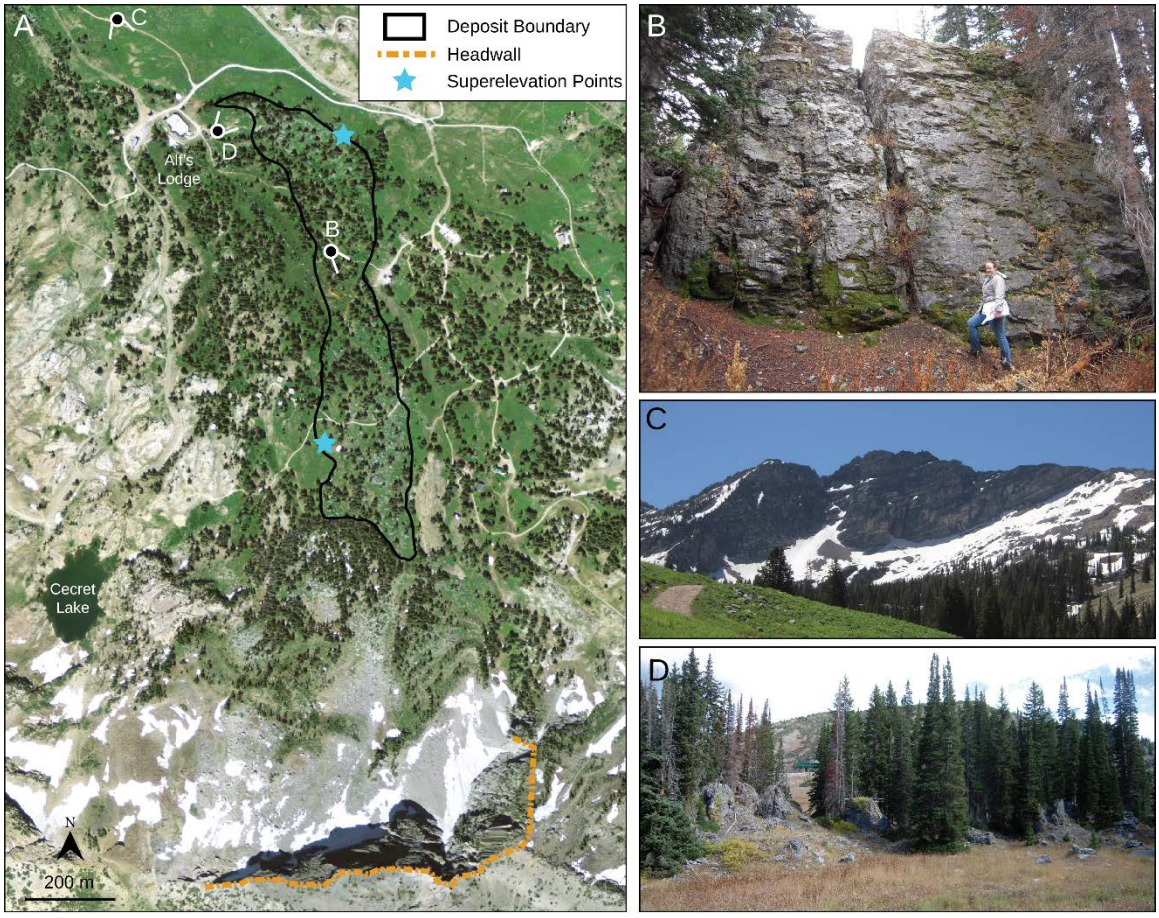

Figure 2
Overview of the study area. Included are mapped boundary and deposit characteristics. A: Mapped rock avalanche deposit in Albion Basin located near Alta, Utah, approximately 20 miles southeast of Salt Lake City, Utah. For clarity only main continuous deposit body is shown. B: Most limestone deposit boulders range from 1 to 6 meters high. C: View of Devils Castle looking south. The rock avalanche originated from somewhere along this headwall. D: Typical deposit character. The deposit is found largely in wooded areas. View is looking southeast.

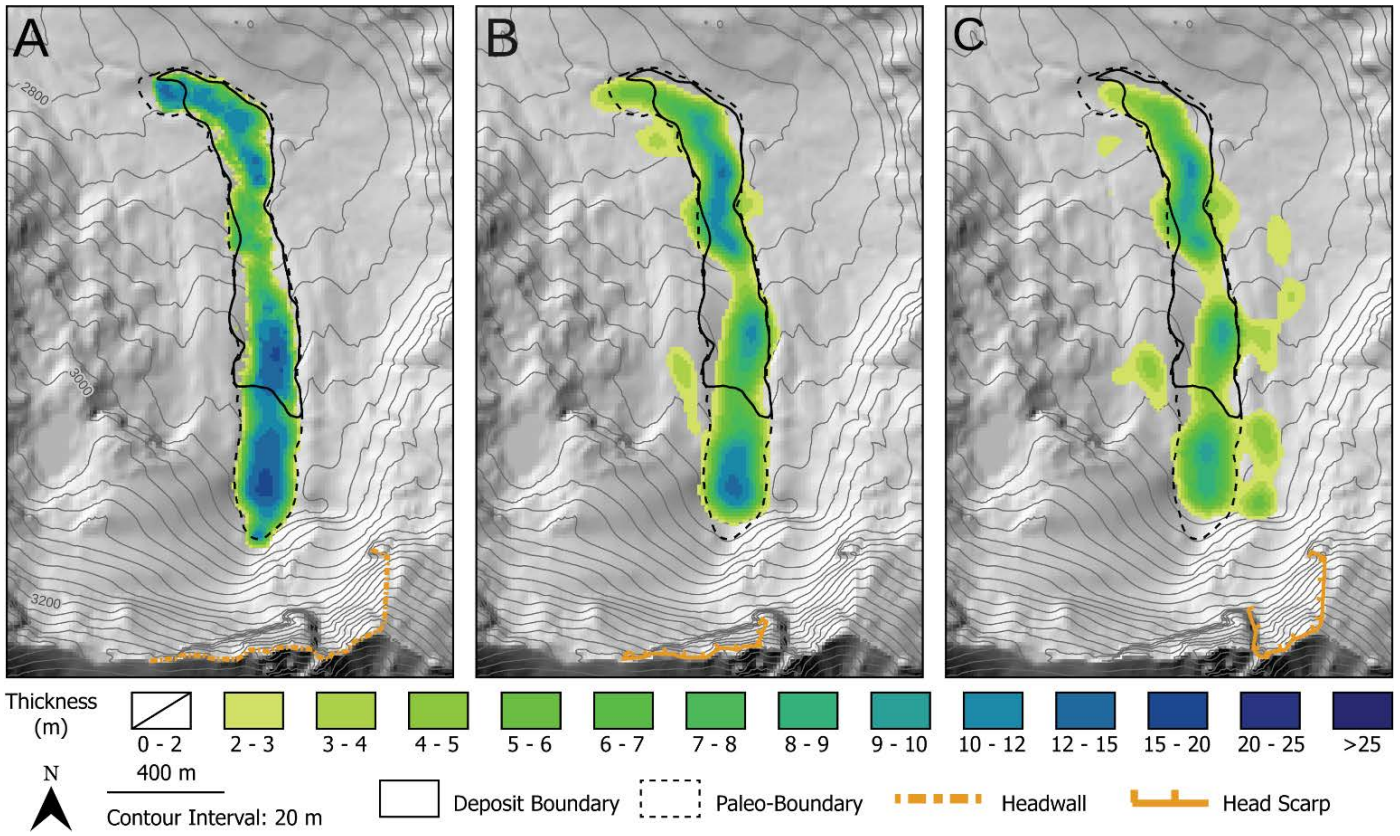

Figure 3
Thickness comparisons of deposit. Results from reconstruction and modeling. A: Estimated thickness of the deposit obtained from topographic reconstruction. B & C: Final runout simulation thickness for the west and east source possibilities, respectively. Runout simulation time for both scenarios is 100 seconds. Final modeled thickness values bulked by 25% for comparison of mapped and reconstructed values. Paleoboundary is the estimated boundary of the original deposit.

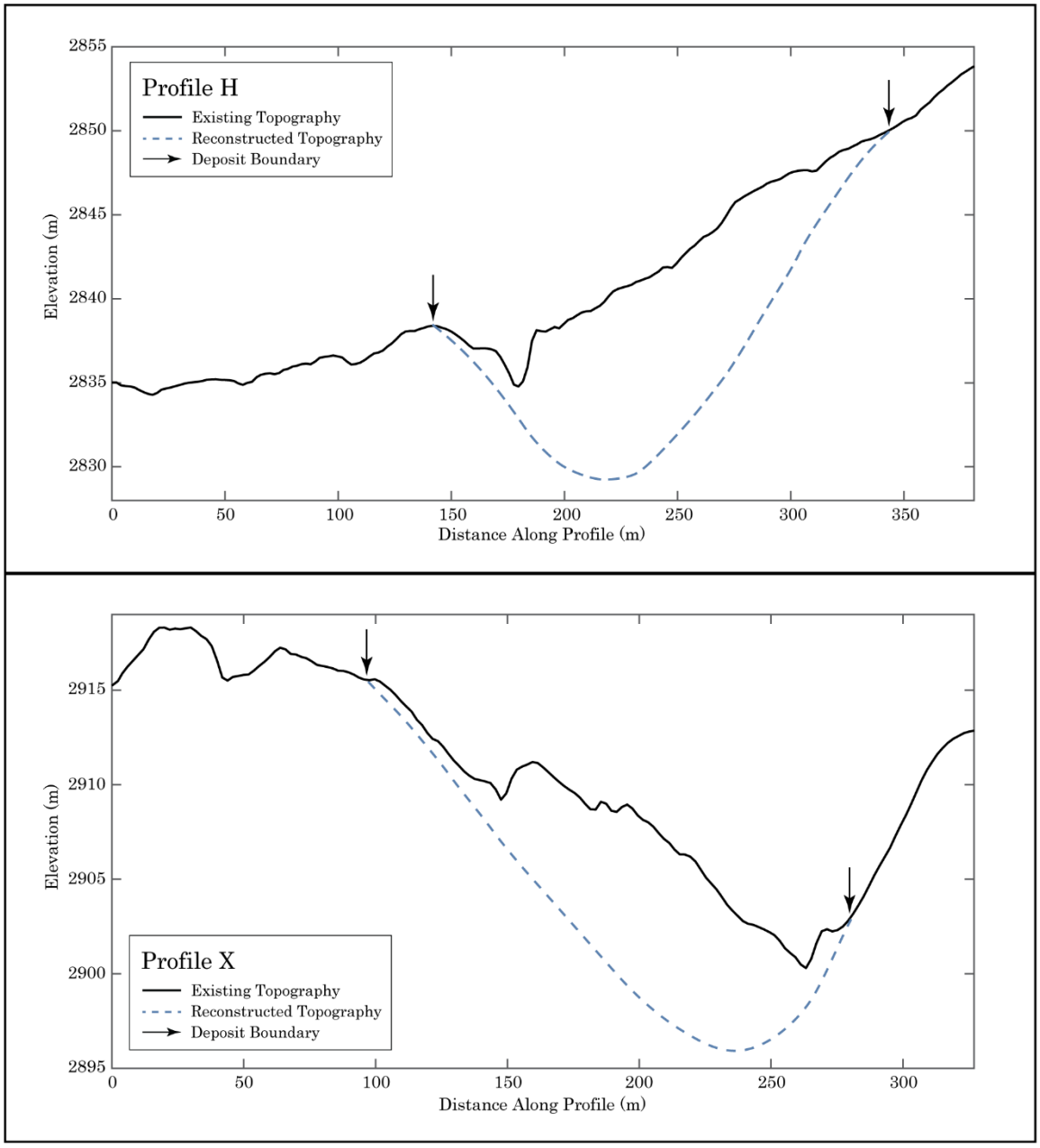

Figure 4
Superelevation profile examples. Elevation axis has been exaggerated for ease of examination. Each profile shows evidence of superelevation in the deposit. Upper panel: Profile H; Lower panel: Profile X. See appendix for profile location.

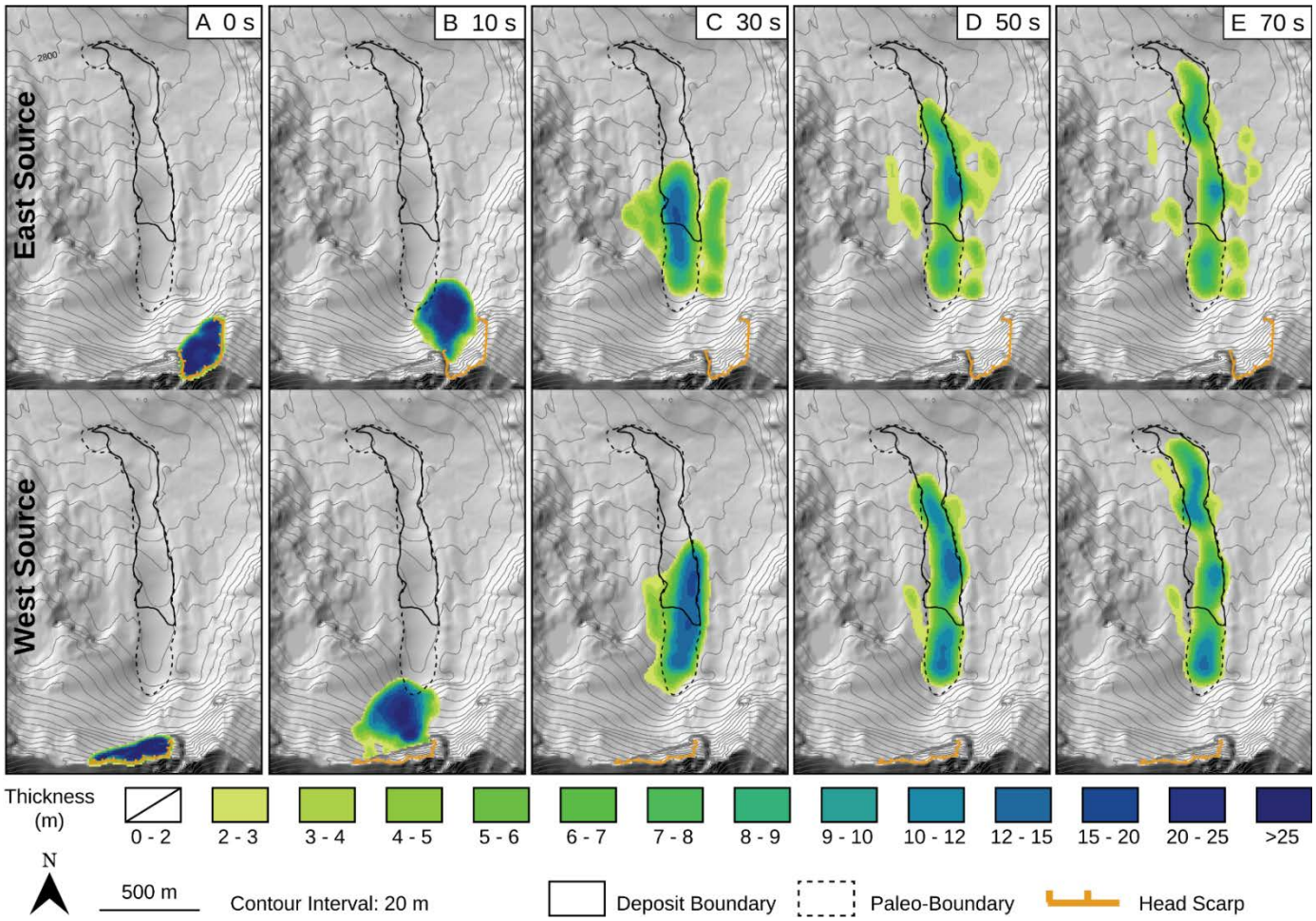

Figure 5
Model dynamics comparison. Panels A–E represent a snapshot of the model at the indicated time in seconds. Top row: east source; Bottom row: west source.

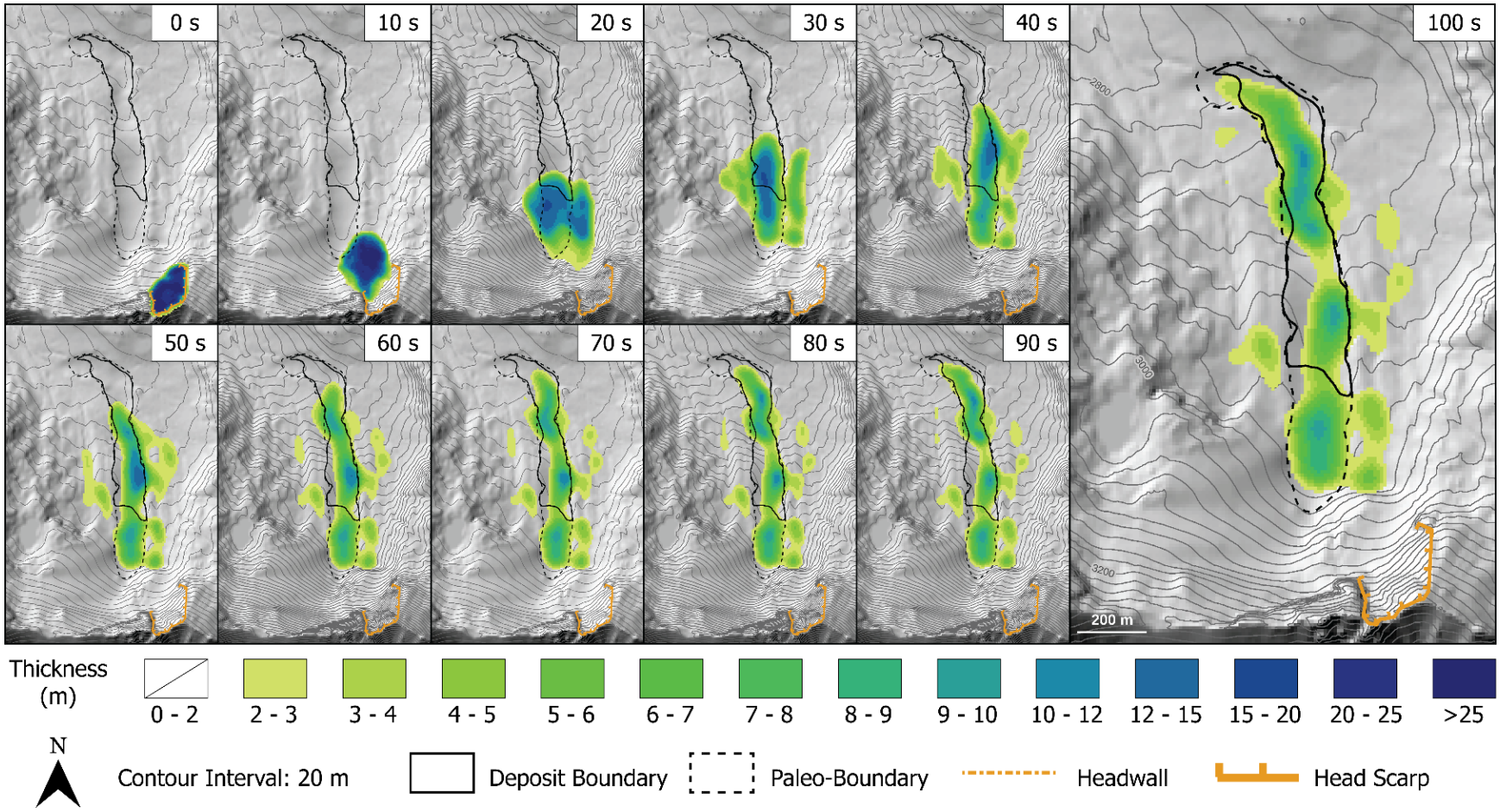

Figure 6
Detail of east source time series. Panels present modeled deposit thickness at the indicated time in seconds.

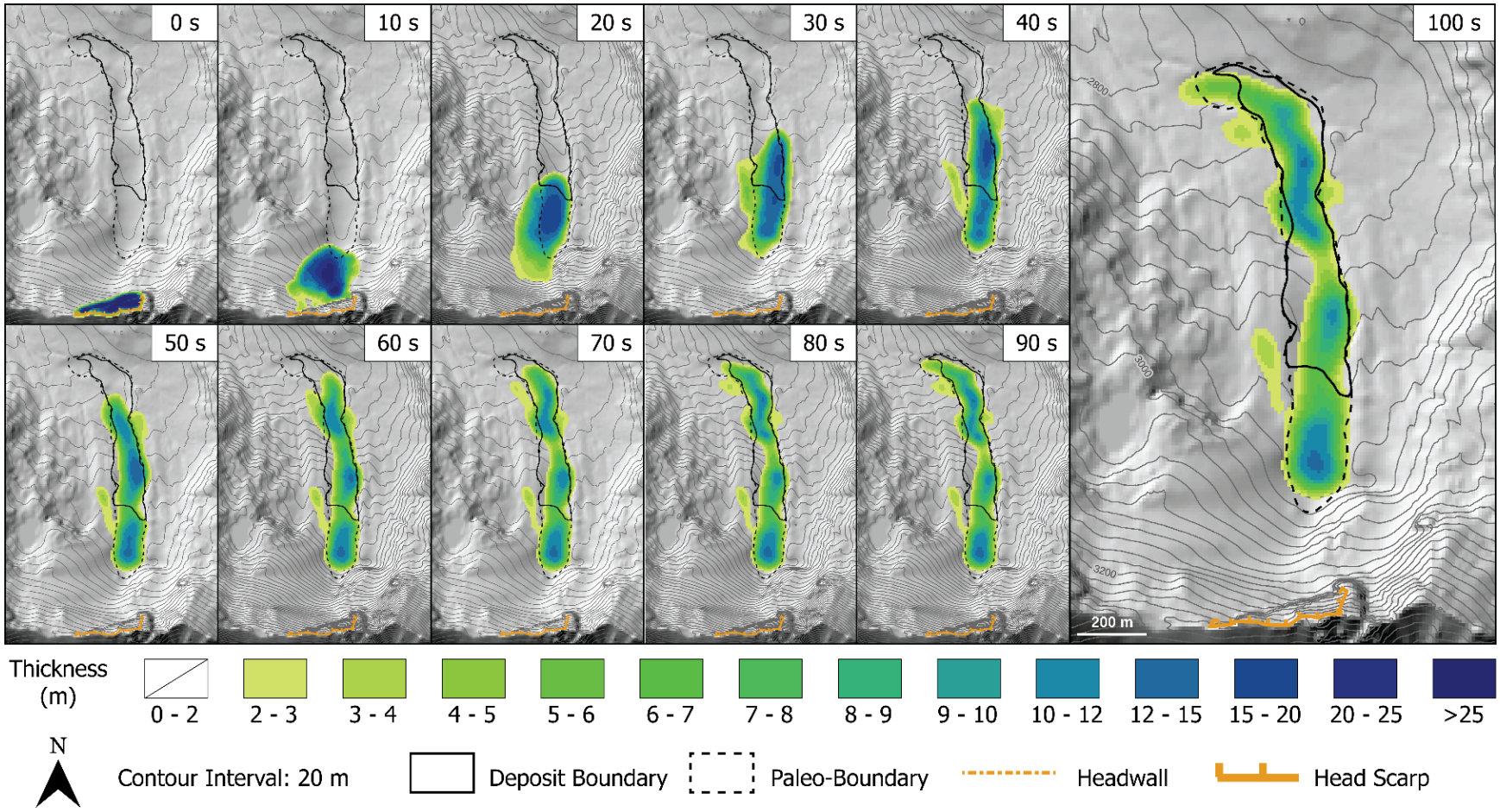

Figure 7
Detail of west source time series. Panels present modeled deposit thickness at the indicated time in seconds.

Table 1

Summary of Parameters Used in DAN3D

Variable	Value
Unit Weight	22 kN/m^3
Friction Coefficient, *f*	0.09
Turbulence Coefficient, ξ	300 m/s^2
Internal Friction Angle	35^o

DISCUSSION

Deposit Description

The two main lithologies comprising the Devils Castle headwall are the Fitchville Formation and the Deseret/Gardison Limestone (Figure 1) (Baker et al., 1966). The Fitchville Formation consists of parallel and persistent cliff forming limestone beds. The Deseret/Gardison Limestone, on the other hand, is more highly fractured and weathered, forming short cliffs and intervening ledges vegetated with pine trees. While observing boulders in the field, Fitchville limestone tends to create a boulder with parallel bedding planes which are clearly seen as opposed to Deseret/Gardison boulders witch have a more weathered, crumbling appearance. A fault cuts through the cliff face forcing the Fitchville to abut the Deseret/Gardison through an up-thrown block (Figure 1) (Baker et al., 1966). As noted, boulders of the rock avalanche deposit are typically weathered, often with a broken and crumbled appearance that mimics the Deseret/Gardison Limestone of the Devils Castle headwall. Boulders of the Fitchville Formation can be found within the rock avalanche deposit, but these occur most frequently on the periglacial feature that overrides the deposit, and

rarely within the main body. Comparing the lithologies of the east and the west source areas (Figure 1), we note that the east source consists mainly of the Deseret/Gardison Limestone, whereas the west source has a large outcrop of Fitchville Formation in the lower part of the cliff face (Figure 1). If the rock avalanche originated from the west source, we would expect to find boulders of the deposit reflect the lithology of the cliff, i.e., a large proportion of Fitchville Formation. However, as mentioned, this lithology is generally missing from the deposit.

Above the main body of the rock avalanche deposit, we mapped glacial and paraglacially modified deposits including large- and low-relief moraines, and a possible rock glacier (Figure 1). These younger deposit features represent a complex history of Lateglacial climate change and landscape response, and help bracket the age of the rock avalanche deposit. Low-amplitude moraines outboard of the large, well-preserved loops (Figure 1) likely relate to a recessional period, following which the nested moraines and rock glacier advanced over the rock avalanche deposit.

Volume and Runout

The Devils Castle rock avalanche displays unusually mobile runout for its volume and fall height. Our calculated Fahrboeschung angle of 14° is low when compared to deposits of similar volume (Figure 8), indicating that most landslides of this volume have shorter runout distance. A possible

mechanism that may explain the low Fahrboeschung angle is entrainment of water during runout (Hungr and Evans, 2004; Dufresne, 2009). We hypothesize that there may have been a small cirque lake at the top of the basin, which when overrun by the rock avalanche was entrained into the debris, increasing the rock avalanche mobility. Cecret Lake, located less than 1 km to the west, provides an example for the scale of such a lake (Figure 2a). There are additional factors that may have influenced the rock avalanche mobility, such as runout over glacial ice. The well-developed nested moraines tucked near the headwall and superimposed on the rock avalanche deposit, indicate that glacier ice may have been present during the failure. Runout over ice would boost mobility (Favreau et al., 2010; Deline et al., 2014), but would also likely lead to spreading of the rock avalanche debris, the latter contrasting with the tightly constrained deposit we mapped.

The Devils Castle rock avalanche deposit is relatively narrow and long, and constrained by only low-relief topography. Rock avalanche deposits tend to spread over low-angle terrain (Grämiger et al., 2016). However, in this case a low-amplitude preslide gully, between 10 and 25 m in depth, was sufficient to trap the debris and dictate the course of runout. This further speaks to a possible high fluid content for the rock avalanche aided by entrainment of water from a cirque lake. The abrupt termination of the deposit at its toe is also notable in spite of the generally low-angle topography. We carefully inspected the drainage farther downstream of the

deposit, and did not discover any evidence of rock avalanche debris, suggesting the deposit terminates at its mapped location.

When large, intact rock masses collapse and fluidize, they undergo a fragmentation bulking process (Hungr and Evans, 2004) that increases their initial volume. In order to recreate the topography of the source area, we accounted for this fragmentation by debulking the calculated deposit volume of 1.7×10^6 m^3 by 25%, a typical fragmentation volume change (Hungr and Evans, 2004; Sherard et al., 1963), which also reflects our chosen bulk density of 22 kN/m^3 for runout simulation (Table 1). This resulted in an estimated initial source volume of 1.36×10^6 m^3. Selecting a different bulking factor would require us to either know the global bulk density of the rock avalanche deposit or have an independent measure of the source volume (which we do not have). Increasing or decreasing the assumed bulking factor would lead to an equivalent change in estimated source volume. We believe the assumed fragmentation bulking factor may reasonably vary within ±5%, giving a source volume range of $1.3–1.4 \times 10^6$ m^3. We assumed no entrainment of additional colluvial or glacial material between the source and deposit. There was no observable or geological evidence of entrainment (cf. Hungr and Evans, 2004).

The largest source of error in our volume calculation likely arises from the topographic reconstruction. However, this error is difficult to quantify. A small change of ±2 m in the mean recreated paleovalley depth, for example,

could result in volume change of ±29%. Moreover, the upper part of the deposit is concealed by superposed glacial and periglacial deposits and talus, which makes determining the precise extents (and shape of former topography) difficult. Further, we observed two small, thin lateral deposits located parallel and to the east of the main rock avalanche deposit. These are included in our mapping (Figure 1). However, we did not include their volumes in our calculations. These lateral deposits are no more than 2–3 m thick and have a combined surface area of 41,500 m^2, giving an estimated total volume of 83,000–124,000 m^3 (~6% of the deposit volume). Also not included in our volume calculation is material loss from the rock avalanche surface by postslide erosion. Throughout the deposit, and seen especially in profiles F–L and W–Z (see Appendix), the stream has eroded a small gully. We estimate that approximately 95,000 m^3 of the rock avalanche has been removed through erosion, or 5% of the deposit volume. We use these error calculations to estimate ±25% confidence bounds on our reported deposit volume of 1.7×10^6 m^3.

Runout Modeling

The lithology of boulders within the rock avalanche deposit indicates that the event was sourced from the Devils Castle headwall. However, there is no obvious topographic evidence on the headwall to indicate the precise source geometry. We identified two likely possibilities for the source area,

reconstructed each with a plausible prefailure topography, and then simulated the resulting runout. The goal was to extract hazard-relevant parameters describing the dynamics of the failure, and potentially evaluate the likelihood of the failure originating from either the east or west source areas.

Runout parameters, such as the selected rheology and values describing basal and internal shear resistance, were identical between models for the east and west source areas, and the results of each model gave similar final values (Figure 3). Both sources successfully channeled the main rock avalanche body into the appropriate strike-gully, and followed the path of the deposit mapped in the field. However, there are differences between the two scenarios regarding thickness and overall distribution of the deposit when compared to our reconstructed values. The east source model matches the mapped extents well, and includes the lateral deposit found to the east of the slide observed in the field (Figure 3c). However, it lacks the depth we estimated from topographic reconstruction. For example, the deepest part we reconstructed is found near the top of the deposit at a depth of over 25 m, whereas the deepest part of the modeled east source deposit in the same area is only 10–12 m. The west source model also matches the mapped extents well, but is missing the upper lateral deposit seen in the field (Figure 3b). Nevertheless, the modeled and reconstructed thickness distributions are similar.

Both east and west source runout models indicated a split from the main rock avalanche body, where a small portion proceeded down a slight side gully that runs parallel and west of the main channel resulting in 2 m thickness of simulated deposit (Figure 3). However, in follow-up field visits, we could not identify evidence of this lateral deposition, and thus believe the result is an artifact of our topographic reconstruction. The area is adjacent to glacial and periglacial deposits that obscure past topography, making reconstruction difficult, and we recreated a gully guided by down-stream topography that seems to have inadvertently funneled some of the deposit to the west, resulting in error.

Since both the east and west source models produced reasonable results, additional field evidence was examined to evaluate which was more viable. Field evidence indicated that the rock avalanche superelevated toward the west near the head of strike-gully (see 20–30 s panel; Figure 6). Analyzing the two runout models, we noted that the east source slide superelevates at this point, whereas the west source slide does not. Field observations further show that a thin layer of boulders is located to the east of the main body (Figure 1). Our east source runout model places boulders in the same spot as observed in the field, whereas the west source model lacks this lateral deposit. Although uncertainties remain, runout modeling and field observations thus suggest that the east source area is the most likely source for the Devils Castle rock avalanche deposit.

Age

We use three pieces of evidence to help bracket the age of the Devils Castle rock avalanche. In a study of glacial till of Little Cottonwood Canyon, Richmond (1964) observed that the rock avalanche age should be bracketed by the middle stade of the Pinedale till, which the deposit overlies, and the late stade, which overlies the deposit. Later, Madsen and Currey (1979) reported two radiocarbon ages from a bog overlying till and landslide debris, taken from a log and oxidized peat, which are 10,571–11,205 cal BP (sample RL-695) and 10,397–11,103 cal BP (sample GX-4736), respectively. Finally, cosmogenic nuclide dating of moraine boulders from recession of the Pinedale glaciation following the Last Glacial Maximum (LGM) reveals that glaciers of Little Cottonwood Canyon began to retreat by ~17,000 years ago (Laabs and Munroe, 2016).

The glacial events described earlier from our field study, in combination with Madsen and Currey's (1979) radiocarbon ages, give a minimum limiting age for the Devils Castle rock avalanche of >10,000 years BP. Then depending on the pace of the glacial recession, which initiated following the LGM but proceeded at an unknown rate to the highest elevations, we can estimate a bracketed age of occurrence of the rock avalanche approximately 11,000 to 16,000 years ago. We are currently awaiting the results from our own cosmogenic nuclide exposure dating of Devils Castle rock avalanche boulders, which should provide an accurate age

for the event that can be compared with limiting age information discussed here.

Preconditioning, Preparatory, and Triggering Factors

The headwall of Devils Castle is complex, carrying a history of preconditioning and preparatory factors that contributed to the rock avalanche. During the Late Pleistocene, climate oscillations drove varying glacier extents in the Albion Basin (Ivy-Ochs et al., 2008). Glacial erosion of the cirque headwall progressively undermined the source area, debuttressing the rock wall and altering stress trajectories (Grämiger et al., 2017), perpetuating internal rock mass damage and conditioning the slope for future failure. Throughout the Late Pleistocene, climate cycles likely continued to prepare the slope for failure. Weathering processes, such as frost cracking (Sanders et al., 2012) or thermo-mechanical fatigue (Gisching et al., 2011), may have contributed to further rock mass damage and progressive failure surface development.

The Wasatch Mountains are situated at the most eastern end of the Basin and Range province in a seismically active region (DuRoss, 2008). An earthquake may thus have triggered the Devils Castle rock avalanche. However, our bracketed range is too broad to correlate with any known paleoearthquakes, and furthermore there is limited information on paleoseismic events prior to 8,000 years ago (DuRoss, 2008). Still, we cannot

rule out the possibility of a seismic trigger due to the active nature of the Wasatch Fault. The rock avalanche may have experienced Salt Lake segment earthquakes between magnitudes 4 and 6.5, which could have triggered a rock avalanche at the epicentral distance (Keefer, 1984). Other triggers for the rock avalanche are also plausible, including snowmelt or rain infiltration, extended cold or exceptionally hot temperatures, but equally feasible is that the event had no recognizable trigger (Collins and Stock, 2016).

Other Rock Avalanches and Implications

The Salt Lake segment of the Wasatch fault is surrounded by ~1 million residents. Records of seismicity on the Wasatch Front indicate there is an 85% chance of a magnitude 5 earthquake occurring within the next 50 years (Wong et al., 2016). With a large portion of the population having built homes near the Wasatch Mountains and surrounding foothills, communities are vulnerable not only to strong ground motion produced by earthquakes, but also to earthquake triggered landslides and landslide dams (Evans et al., 2011). Understanding and detailed characterization of the complete earthquake hazard scenario, including secondary effects such as mass wasting, is critical for mitigating seismic risks.

We identified five other deposits of prehistoric rock avalanches near the Wasatch Front. Table 2 and Figure 9 provide summary information for

these five additional slides including estimated volume and Fahrboeschung angle. These rock avalanches were selected based on their proximity to the Wasatch Fault and other major faults, character of the deposit suggesting very rapid runout velocities, and their size with each being similar to or larger than Devils Castle.

Figure 8 places these slides in the context of world-wide case history data, comparing them to previously studied events. The five Wasatch Front rock avalanches are all large in volume (1×10^6 m^3 to 2×10^7 m^3), three have low Fahrboeschung angles for their respective size (Devils Castle, South Fork, and Grandview Peak), and two have comparably large volumes (Smith and Morehouse and Grandview Peak). Low Fahrboeschung angles and large volume slides produce rock avalanches with high mobility, while the combination of these factors contributes to greater mobility in the case of Grandview Peak. Since these five deposits plus Devils Castle are found close to the Wasatch Front, regardless of how they were triggered, geological evidence shows that large rock avalanches occur and should be considered as a high-magnitude, low-frequency hazard.

Additional hazards related to rock avalanche in steep canyons are landslide dams, which may impound large volumes of water but lack engineered protection such as a core or spillway and are thus prone to catastrophic failure (Evans et al., 2011). Outburst floods resulting from breech of a landslide dam can endanger population centers many kilometers

downstream from the rock avalanche deposit, amplifying the risk associated with these slope failures. Of the six slides studied in this work, four show evidence of having generated landslide dams: South Fork, Smith and Morehouse, Grandview, and White Pine, each having an upstream alluvial plain associated with the deposit (Figure 9A–D). Devils Castle shows evidence of damming a drainage creating the bog just above the toe. However, the volume of impounded water is not large. Nonetheless, if a rock avalanche (or several) occurred coseismically and during a time of high water discharge, landslide dams could pose a high hazard for population along the Wasatch Front.

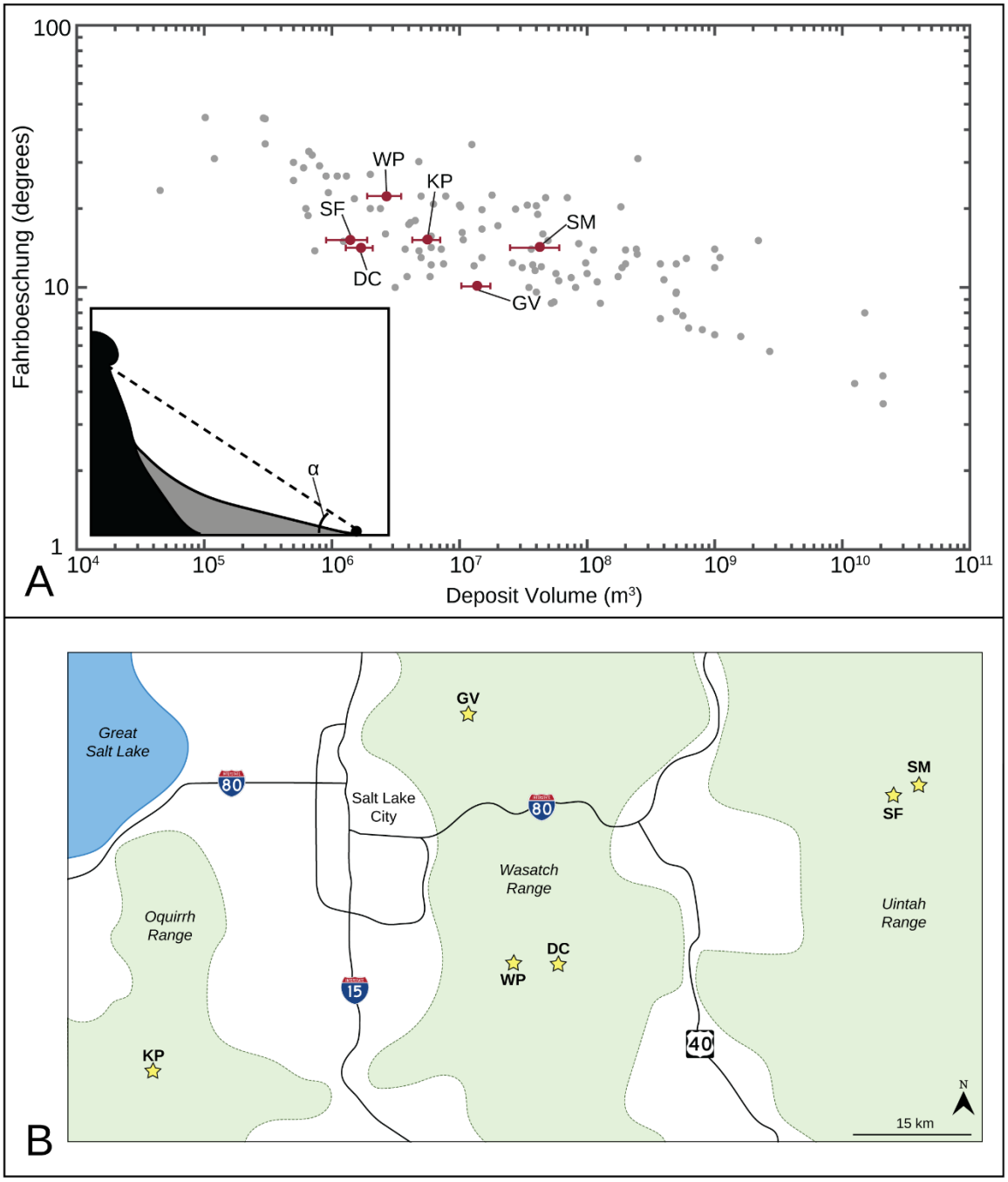

Figure 8
Fahrboeschung vs. volume plot. The plot includes the six rock avalanches found in the region discussed. A: Each slide, including the Devils Castle rock avalanche, has been plotted with other reported landslide events from across the globe (Davidson, 2011). B: Approximate location of the deposits. Smith and Morehouse (SM), White Pine (WP), Kelsey Peak (KP), Devils Castle (DC), South Fork (SF), Grandview (GV).

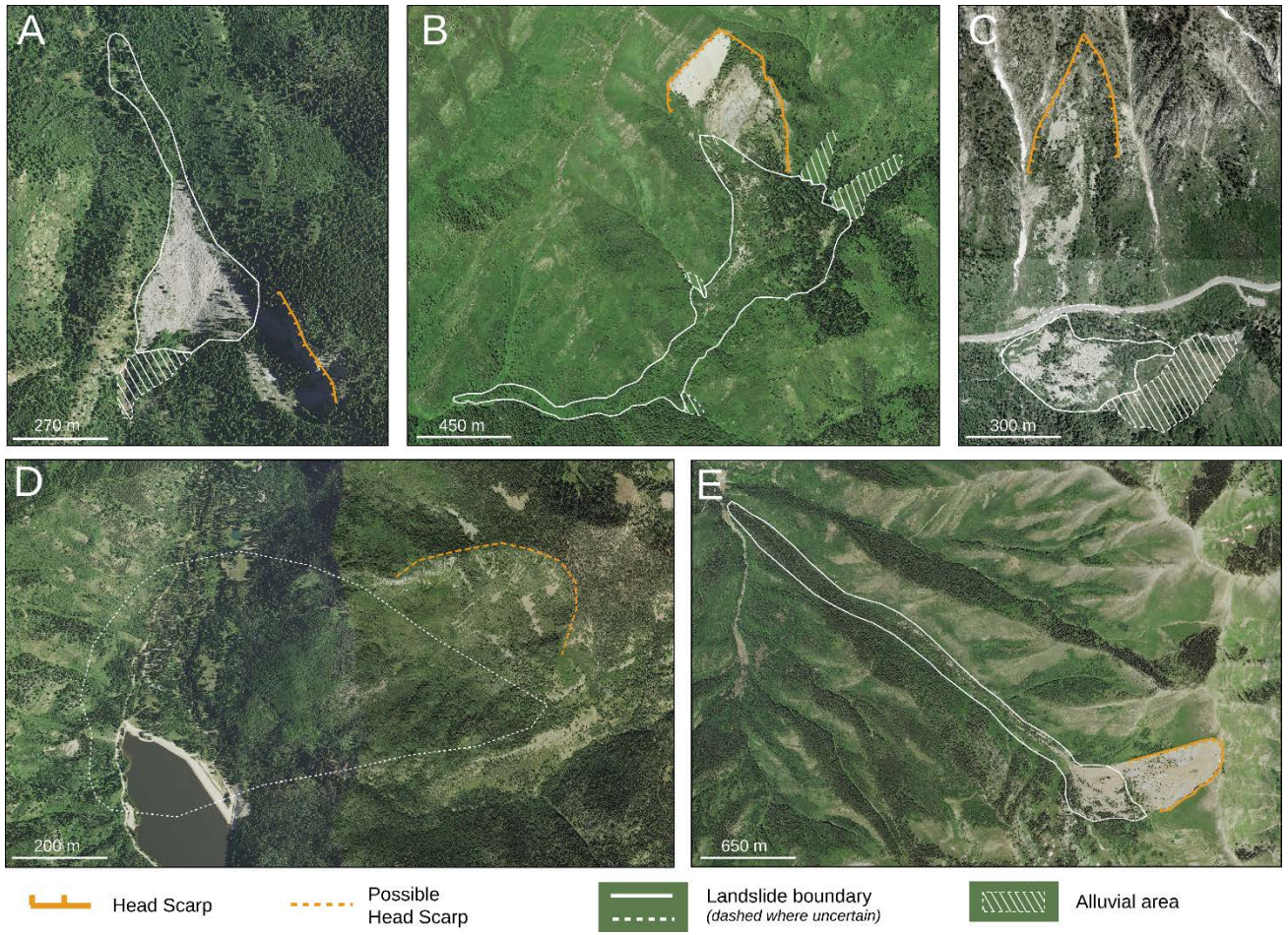

Figure 9
Other rock avalanches found in the region. Each has been mapped with a combination of remote sensing and ground studies. A: South Fork; B: Grandview; C: White Pine; D: Smith and Morehouse; E: Kelsey Peak. Panels A–C contain alluvial deposits collected when the deposit dammed natural drainages.

Table 2

Other Rock Avalanche Information

Slide	ID	Location	Deposit Volume (m^3)	Fahrboeschung (°)
Devils Castle	DC	N 40.579 W 111.616	1.3×10^6 – 2.1×10^6	14
Kelsey Peak	KP	N 40.445 W 112.223	4.3×10^6 – 7.2×10^6	15
Grandview Peak	GV	N 40.844 W 111.748	11×10^6 – 18×10^6	10
Smith and Morehouse	SM	N 40.770 W 111.090	3×10^7 – 6×10^7	14
South Fork	SF	N 40.722 W 111.168	8.8×10^5 – 1.8×10^6	15
White Pine	WP	N 40.574 W 111.688	1.9×10^6 – 3.5×10^6	22

CONCLUSION

In this study, we presented a detailed case history analysis of the Devils Castle rock avalanche, a high-magnitude, low-frequency landslide characterized by high mobility and fluid-like runout motion. The deposit is located in the Albion Basin, at the head of Little Cottonwood Canyon, near the town of Alta, Utah in the Wasatch Mountains.

The rock avalanche deposit consists mostly of Deseret/Gardison limestone and is ~1.5 km in length, with the visible portion of the deposit being 1 km, and the source-proximal debris being obscured by younger glacial and periglacial deposits near the headwall. The calculated Fahrboeschung angle is 14°, and comparison with worldwide values for similar volume events indicates the slide has relatively high mobility. We hypothesize there may have been a small cirque lake at the top of the basin, which when overrun by the rock avalanche increased the mobility through incorporation of water. Through topographic reconstruction and differencing, we calculated a deposit volume of 1.7 million m^3, and accounting for a fragmentation volume change of 25% during failure, we estimated the source volume as 1.3×10^6 m^3. The reconstructed maximum thickness of the deposit is ~25 m, with an average

thickness of 7 m. We estimate a bracketed age of occurrence as 11,000 to 16,000 years from limiting radiometric dates from a peat sample overlying the slide and cosmogenic exposure ages from recessional moraines of the last glacial period.

Field observations of the deposit showed two superelevation points and two thin lateral deposits to the east of the main body. Studying the headwall, we found no obvious evidence to indicate the precise source geometry. After reconstructing two reasonable source areas and running 3D numerical runout simulations for each, we found the results agree well with mapped deposit boundaries for both source scenarios. However, the east source model better represented characteristics of the deposit observed in the field by matching the two superelevation points and a lateral deposit. The east source failure attains a maximum velocity of ~62 m/s, and has two superelevation points closely matching those discovered during field mapping. The upper superelevation point has a modeled velocity of 25–30 m/s, and the lower superelevation point a velocity of 10–15 m/s.

Glacial erosion of the cirque headwall progressively undermined the source area, debuttressing the wall through removal of bedrock and changing stress trajectories over time, likely play a key role in conditioning the slope for future failure. Later climate cycles and environmental weathering processes, in addition to seismicity, likely generated further rock mass damage and contributed to failure surface development.

Rock avalanches are rare phenomena, and because of their scarcity, little information is normally available to describe the hazard posed by these events. Geologic records provide key data to characterize this hazard. Combining results from this study with information we gathered for five additional, similar events around the Wasatch Front, we provide key data needed to evaluate the risk posed by this rare and potentially destructive type of mass movement. Each of the events we describe occurred near the Wasatch Fault, and together with the possible coupled hazard of landslide dam formation, may represent an important aspect of earthquake hazard scenarios requiring explicit treatment.

APPENDIX

RECONSTRUCTION PROFILES

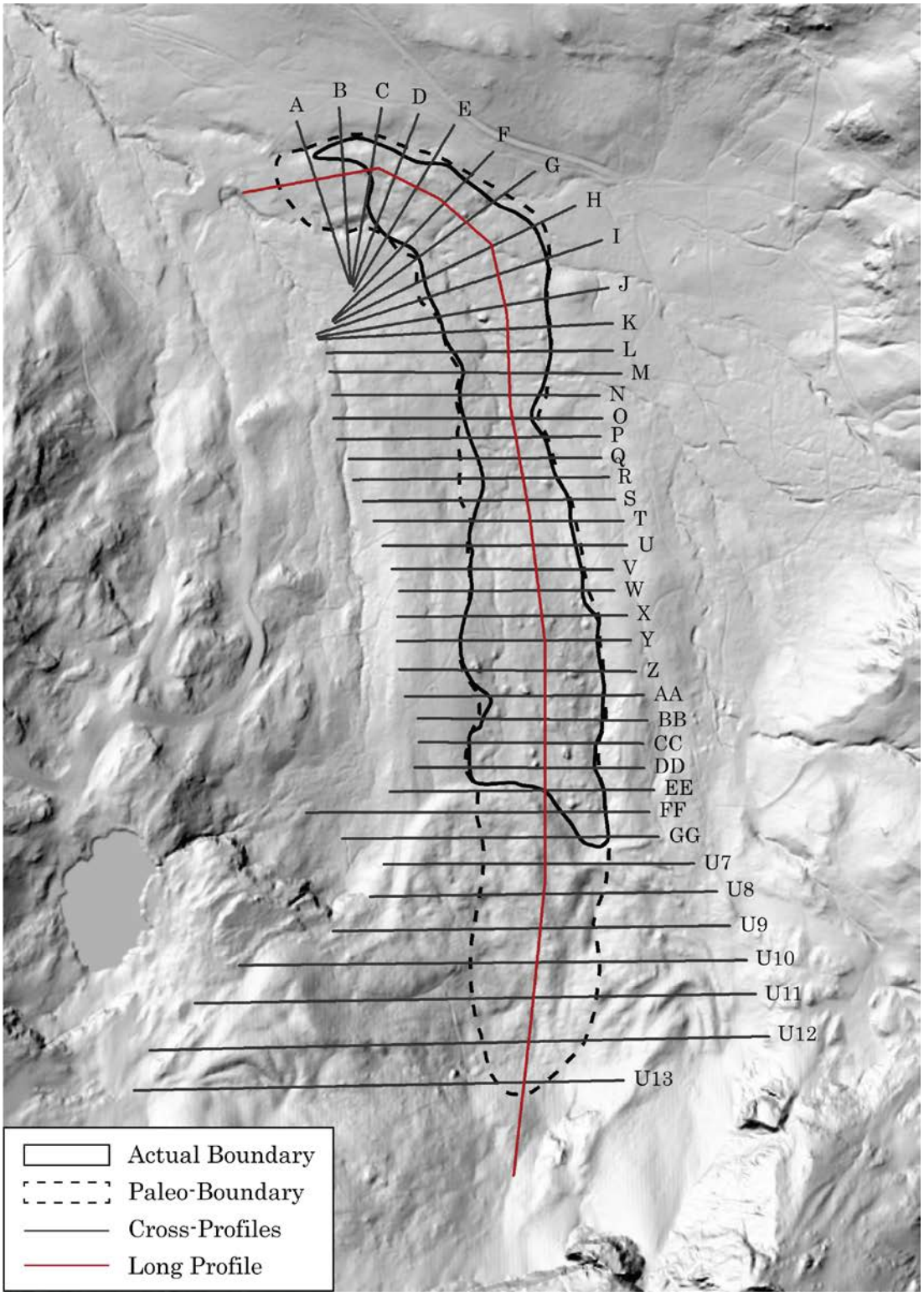

Figure 10
Profile location map

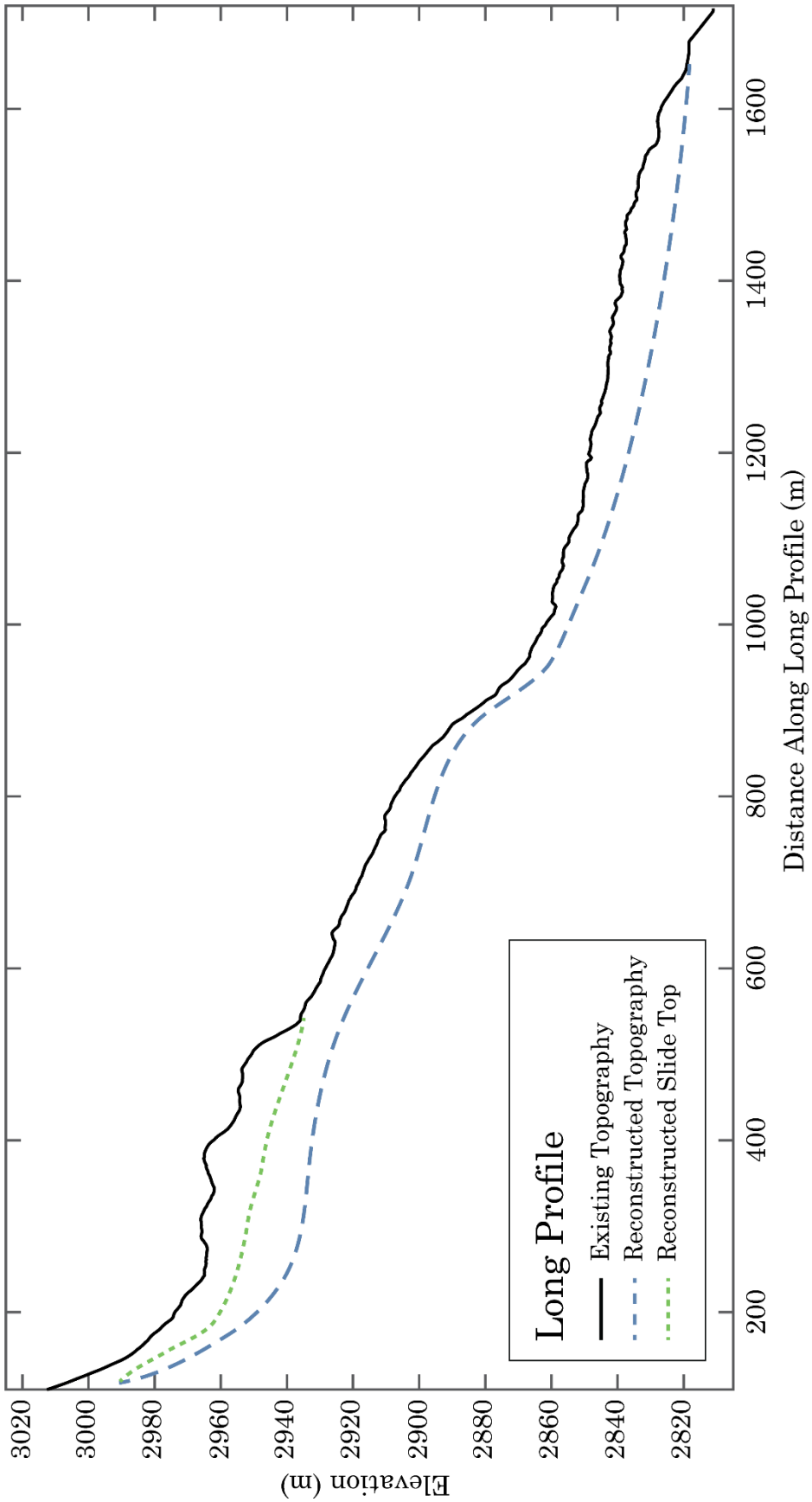

Figure 11
Long profile of deposit. The long profile includes existing topography, reconstructed topography and the reconstructed slide top.

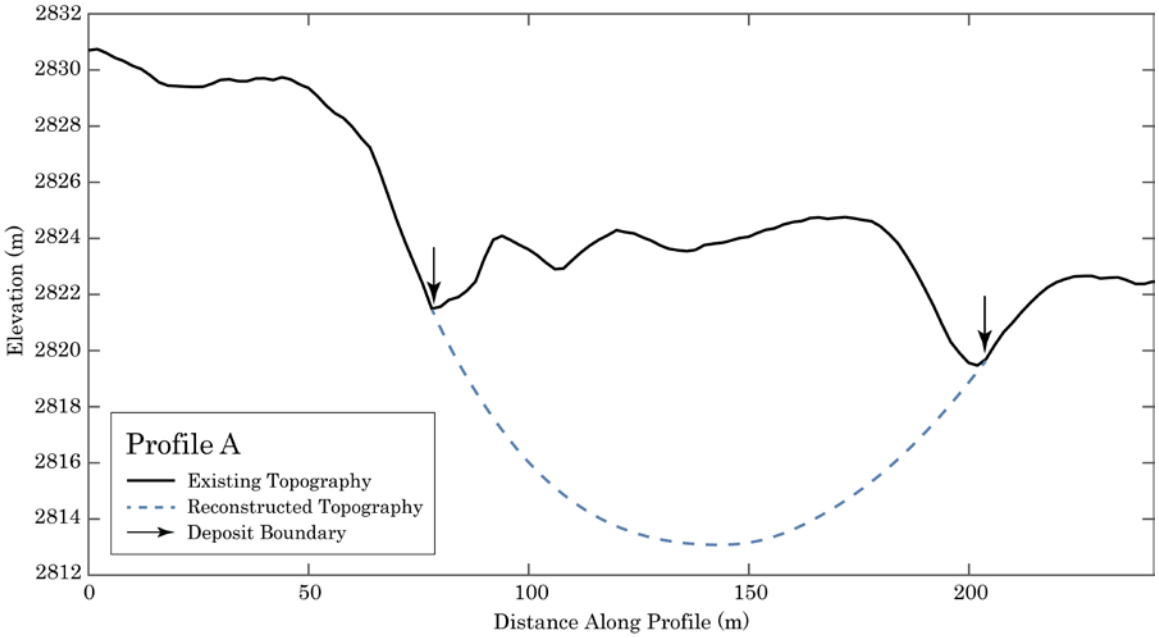

Figure 12
Profile A

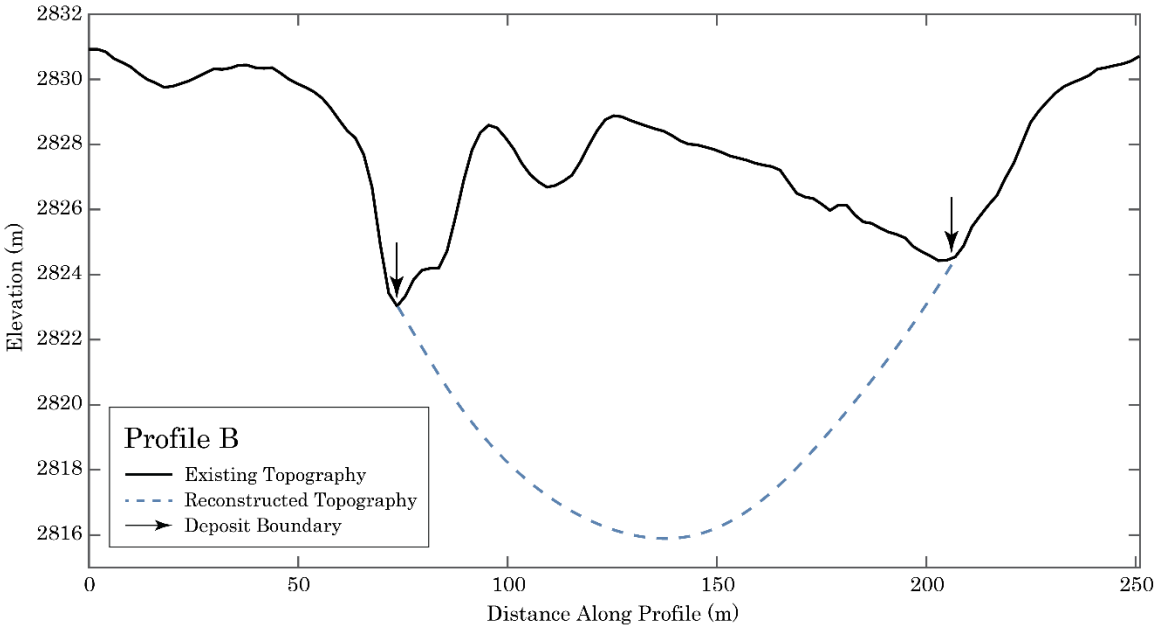

Figure 13
Profile B

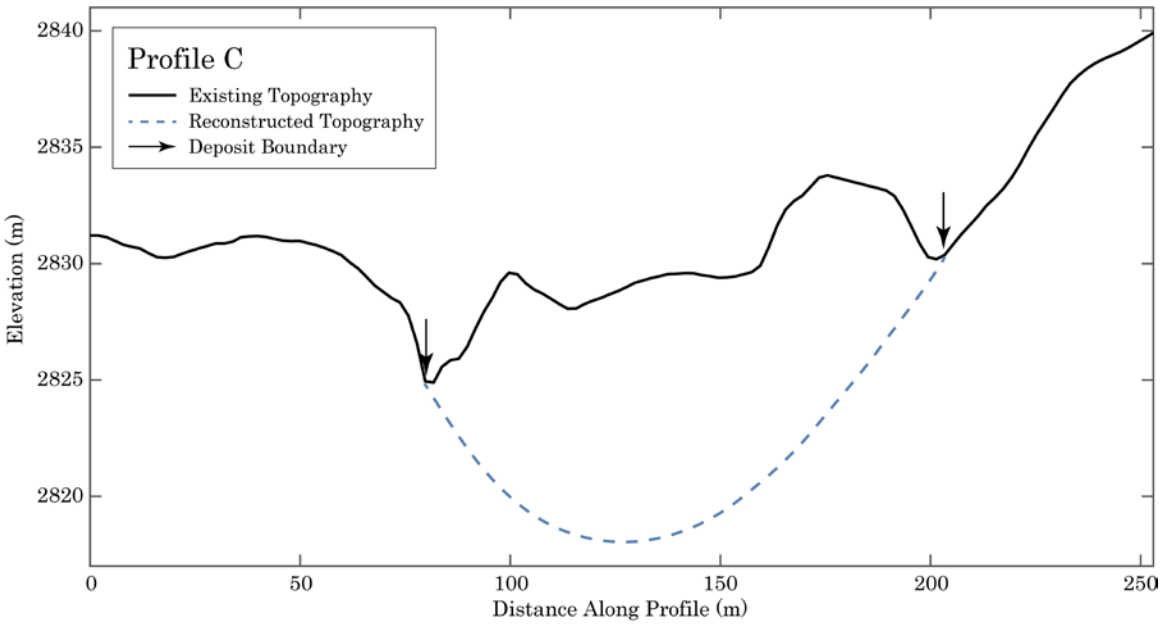

Figure 14
Profile C

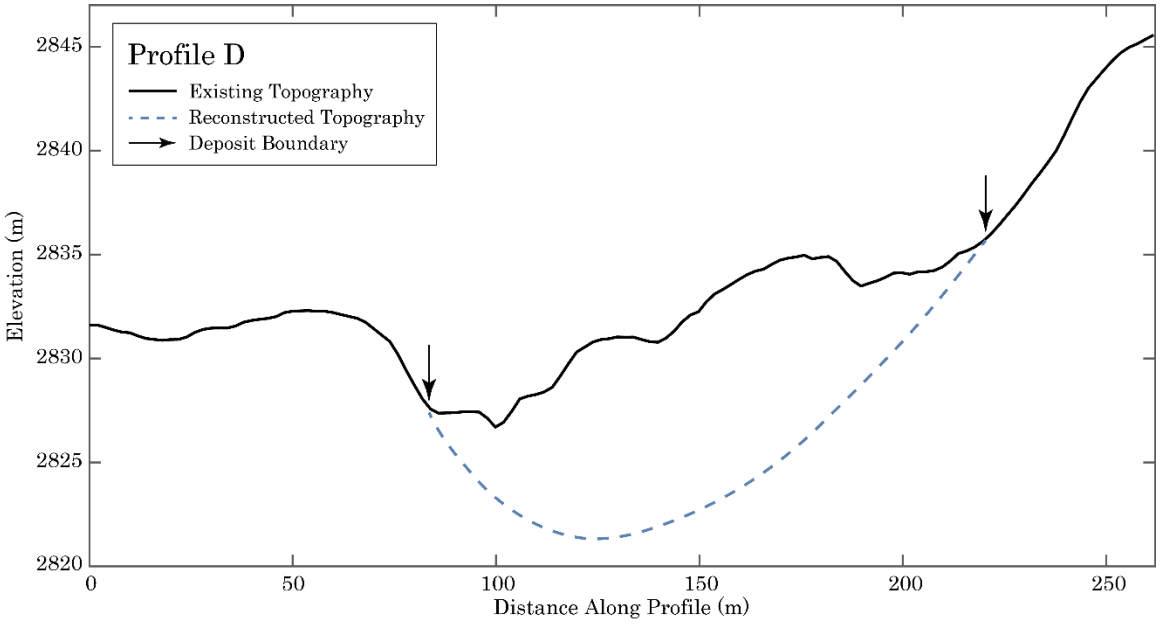

Figure 15
Profile D

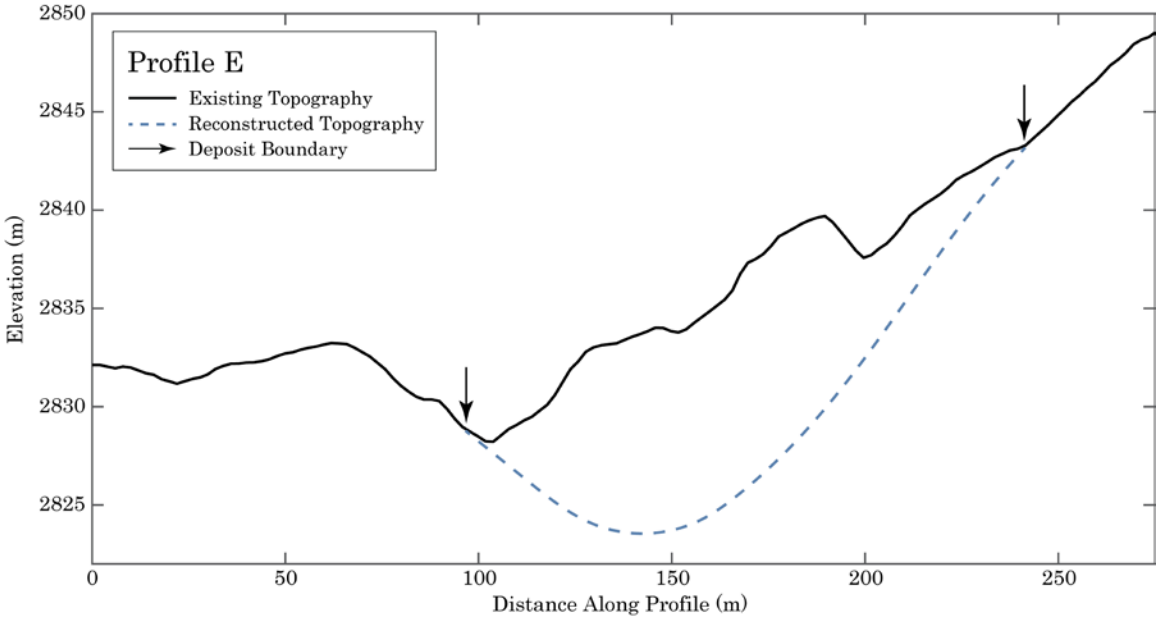

Figure 16
Profile E

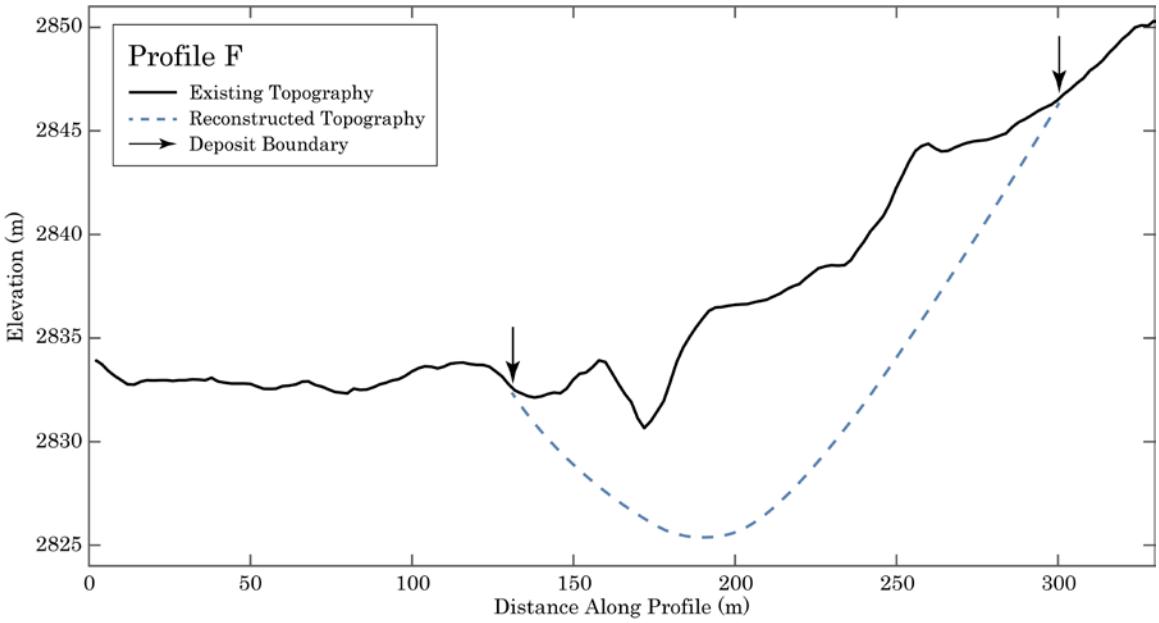

Figure 17
Profile F

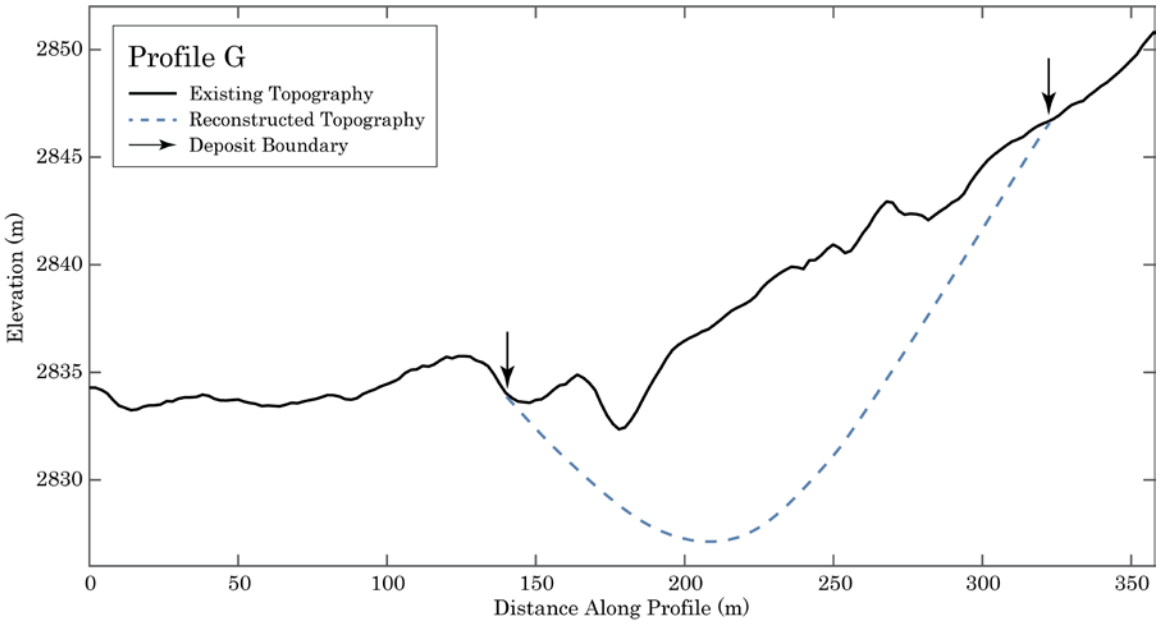

Figure 18
Profile G

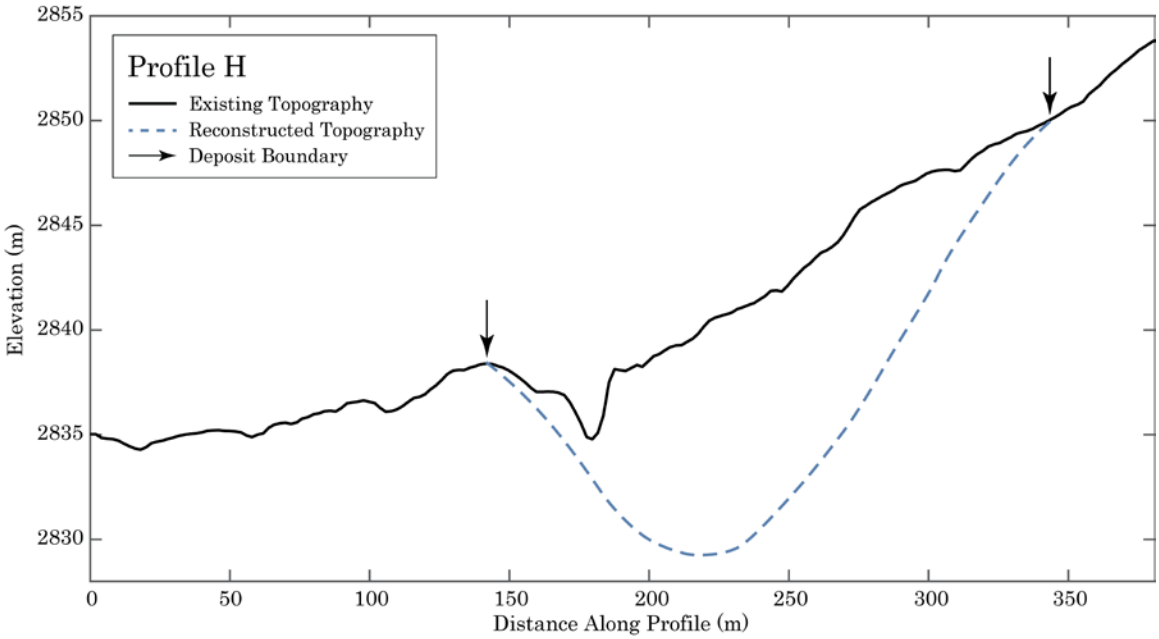

Figure 19
Profile H

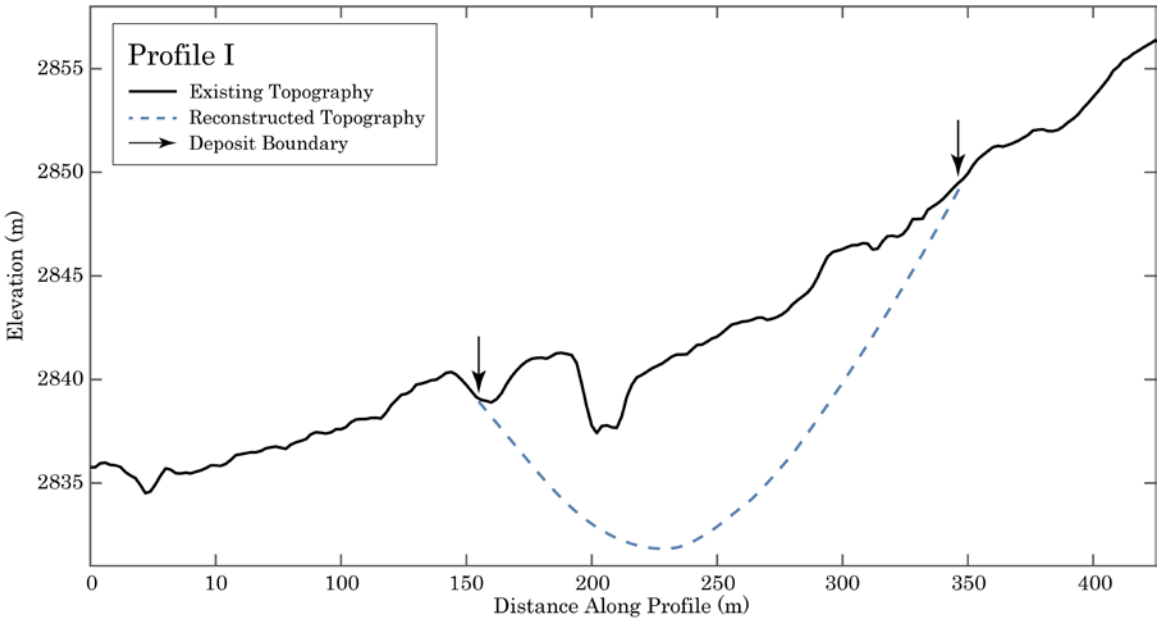

Figure 20
Profile I

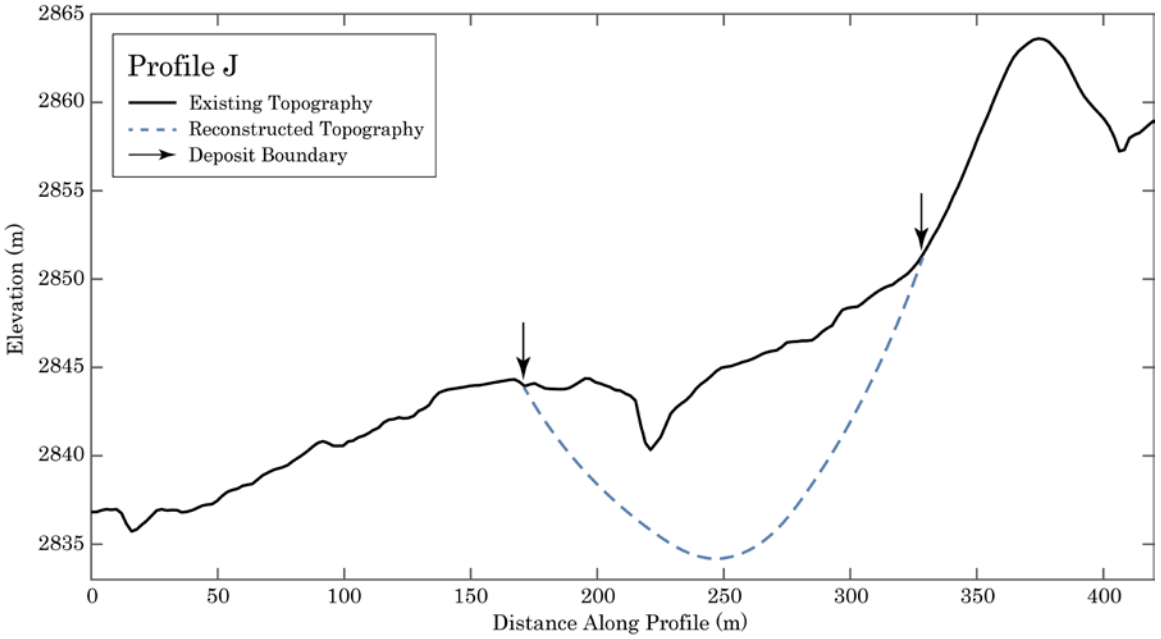

Figure 21
Profile J

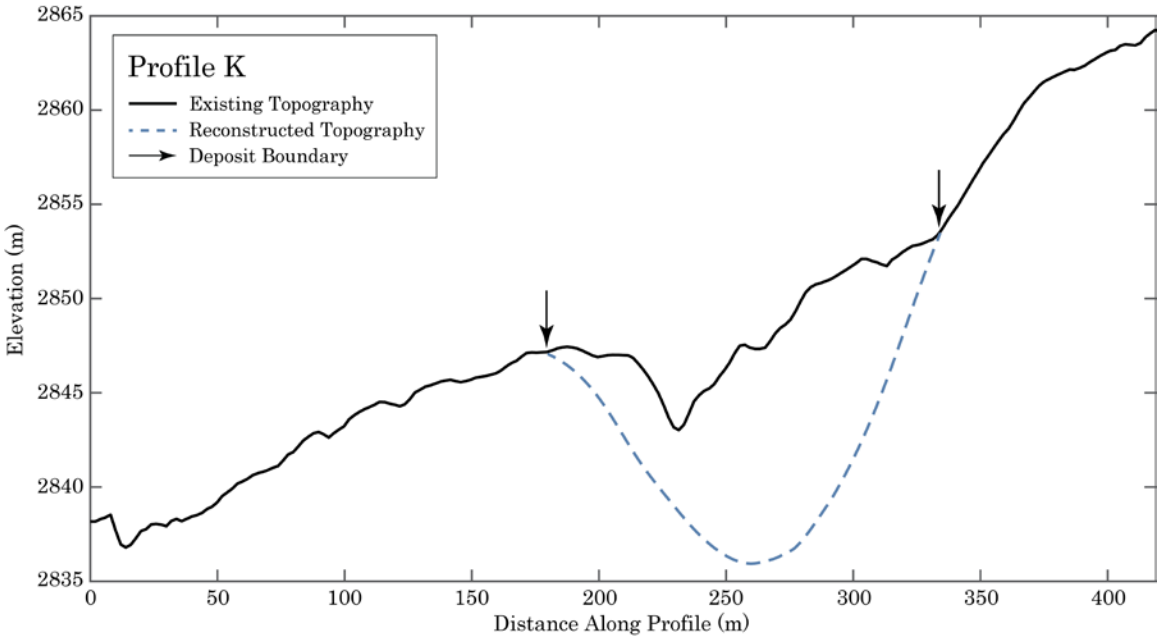

Figure 22
Profile K

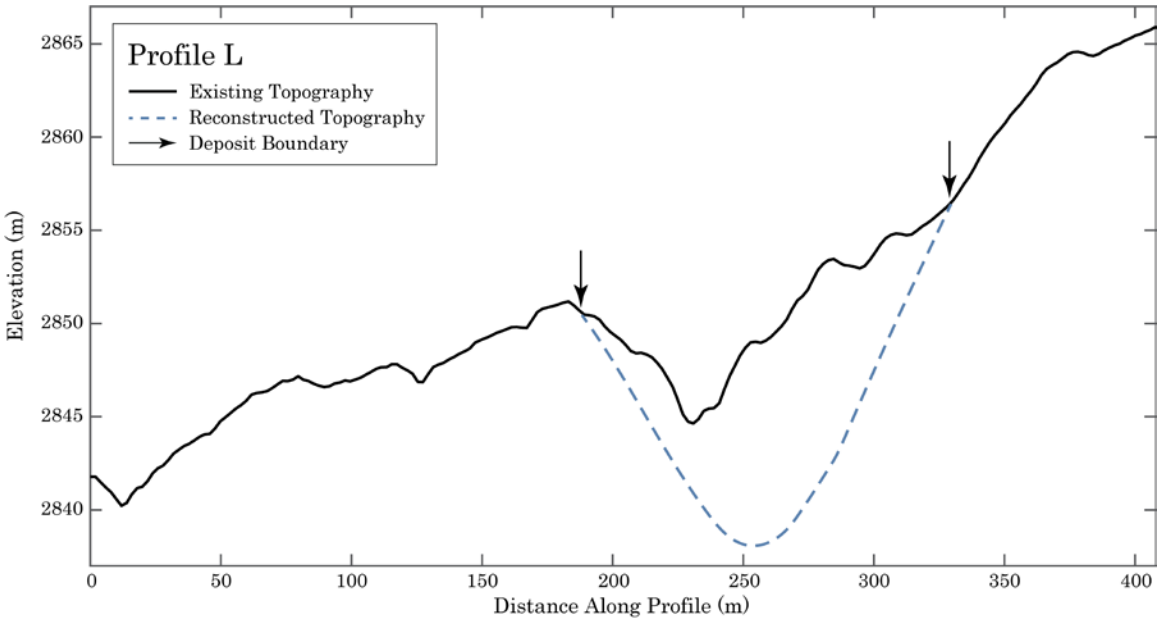

Figure 23
Profile L

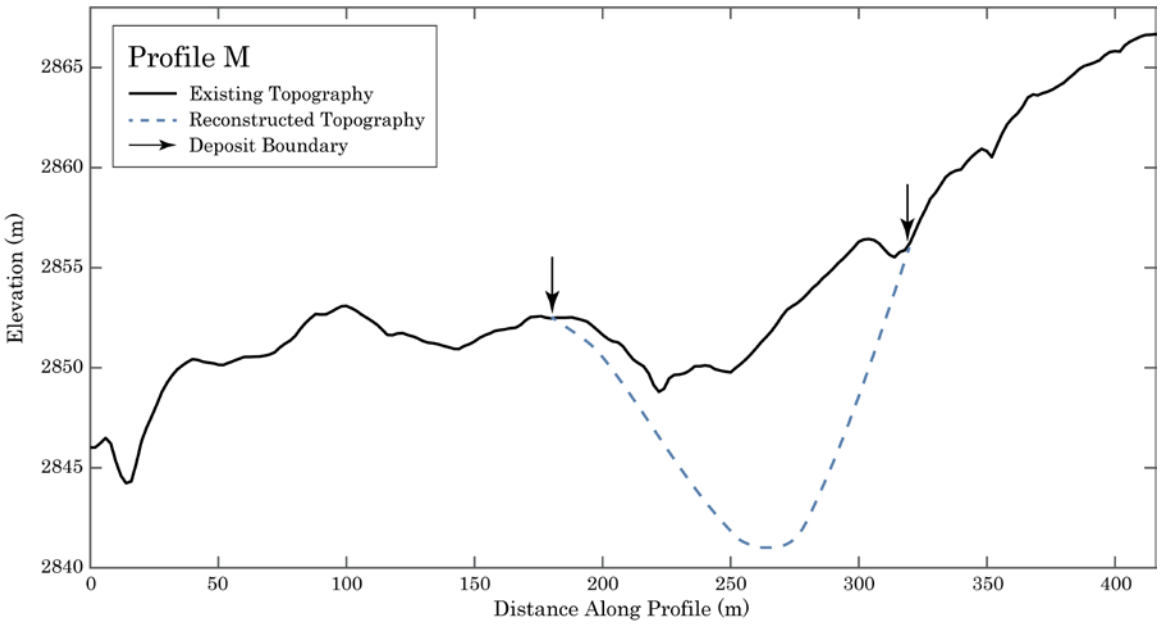

Figure 24
Profile M

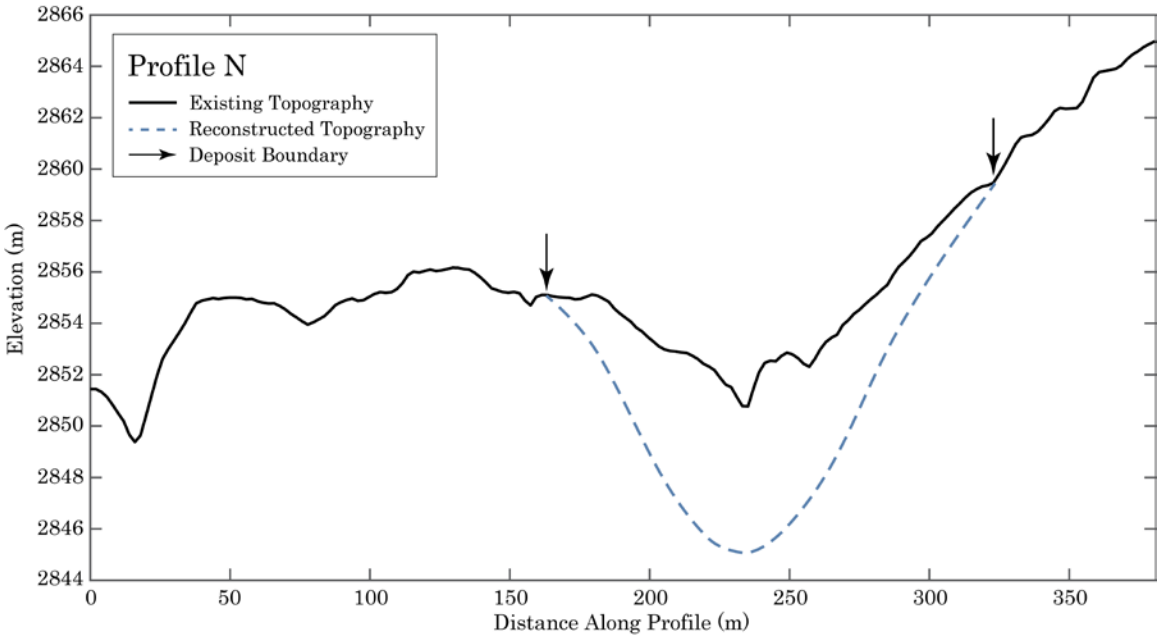

Figure 25
Profile N

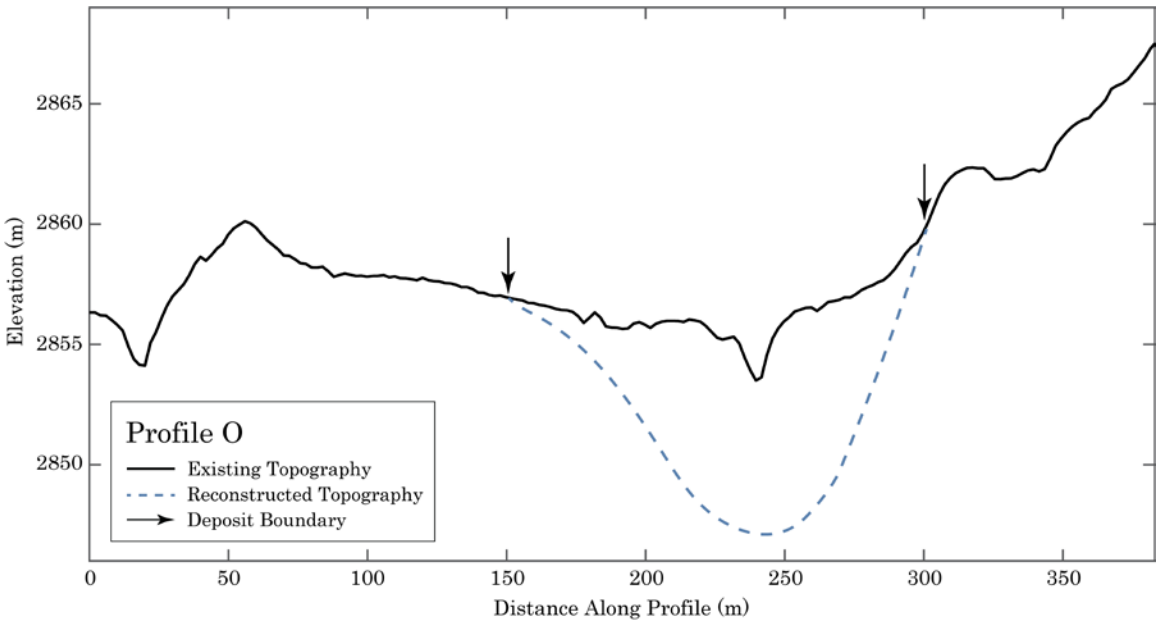

Figure 26
Profile O

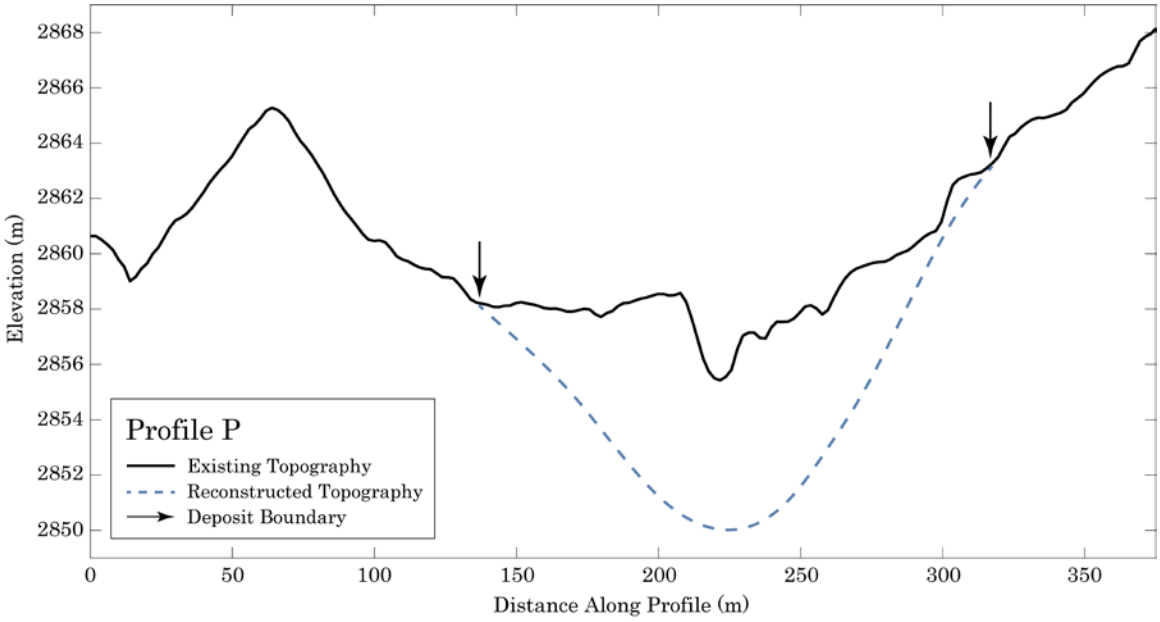

Figure 27
Profile P

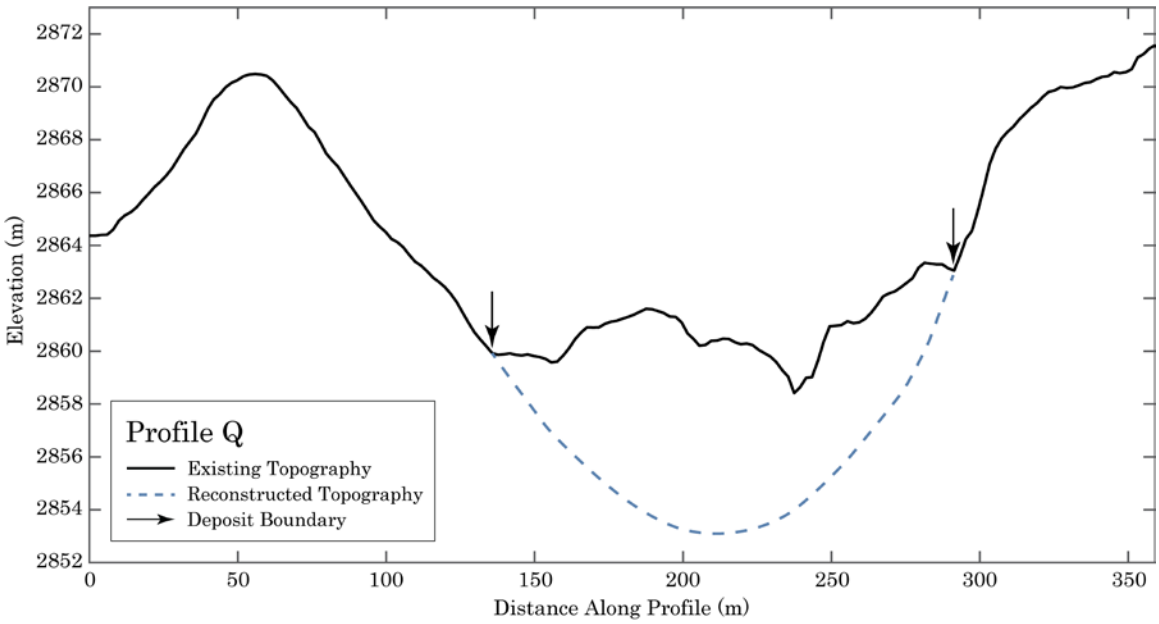

Figure 28
Profile Q

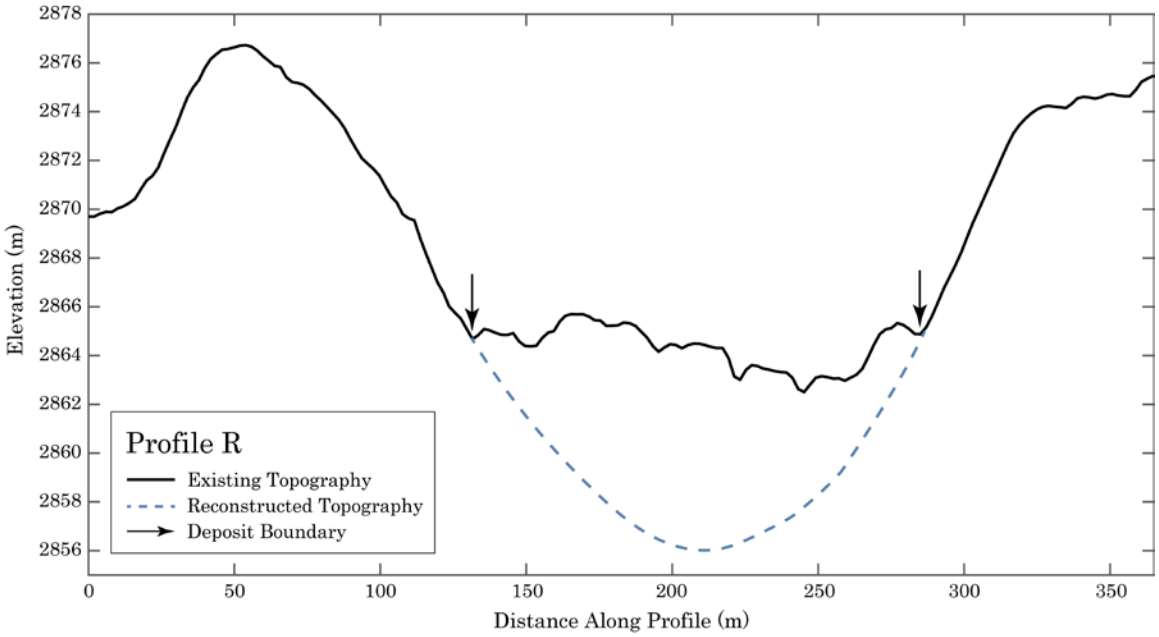

Figure 29
Profile R

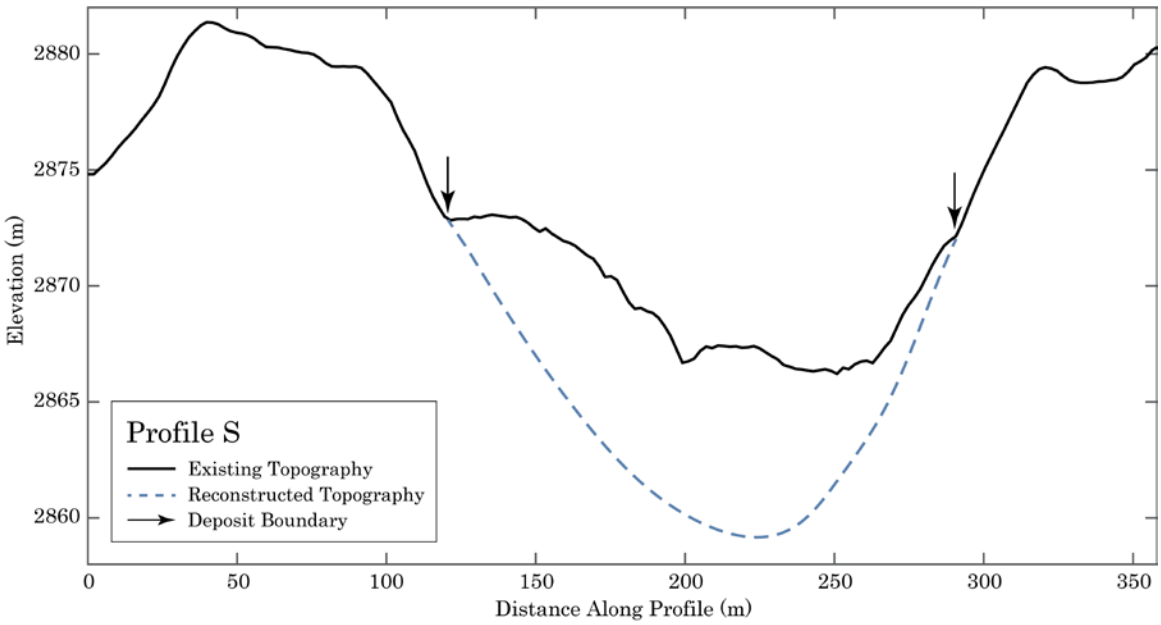

Figure 30
Profile S

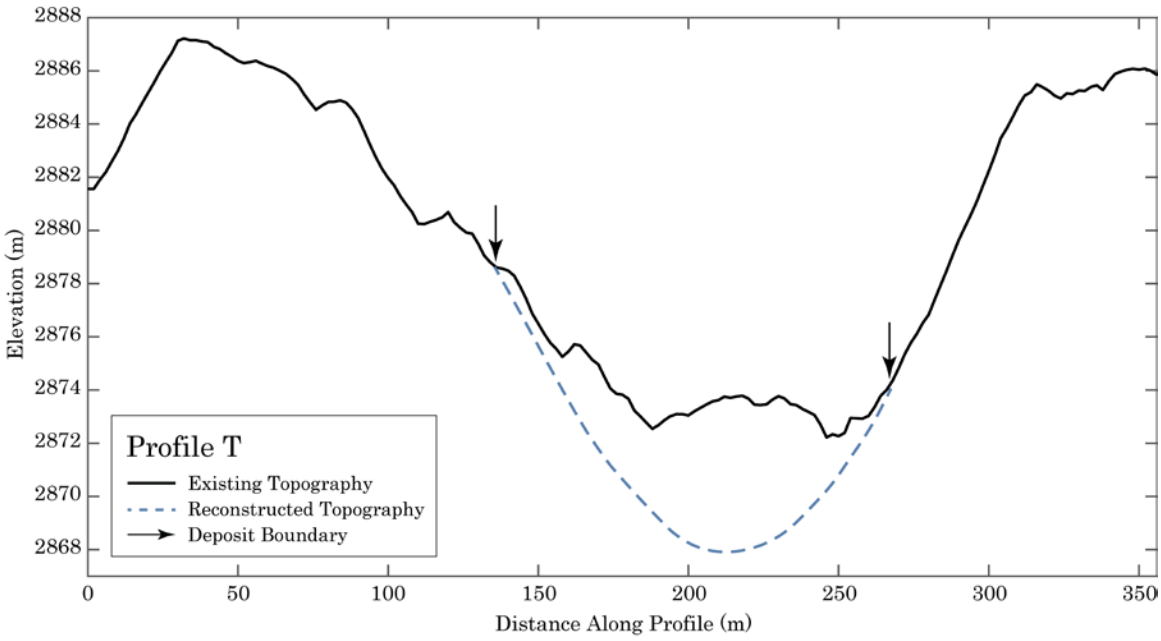

Figure 31
Profile T

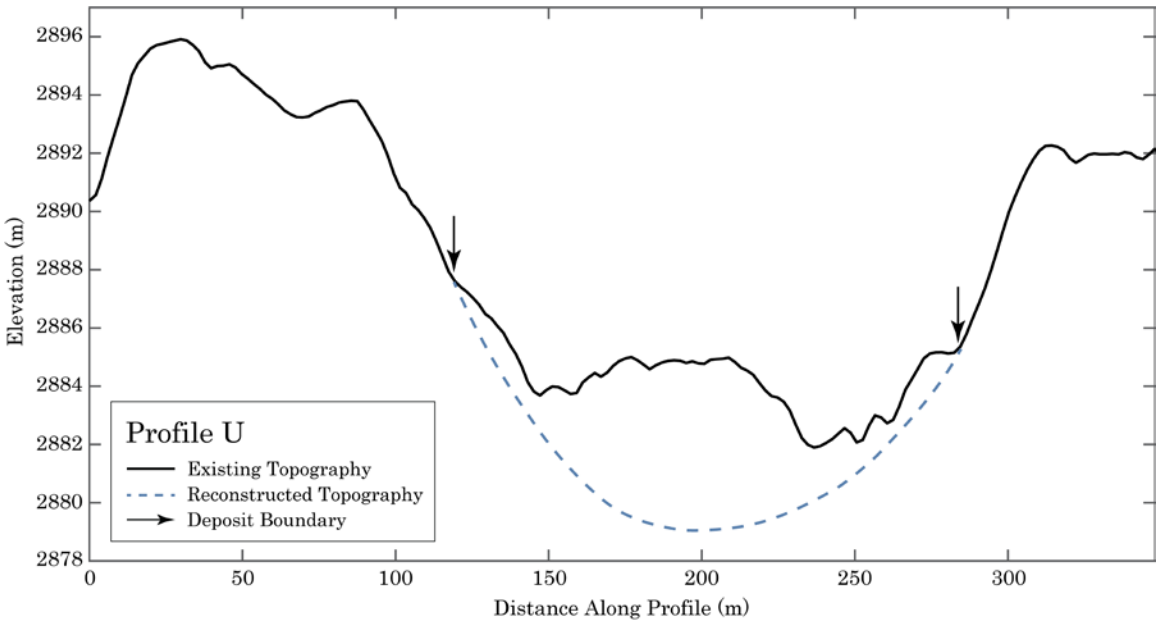

Figure 32
Profile U

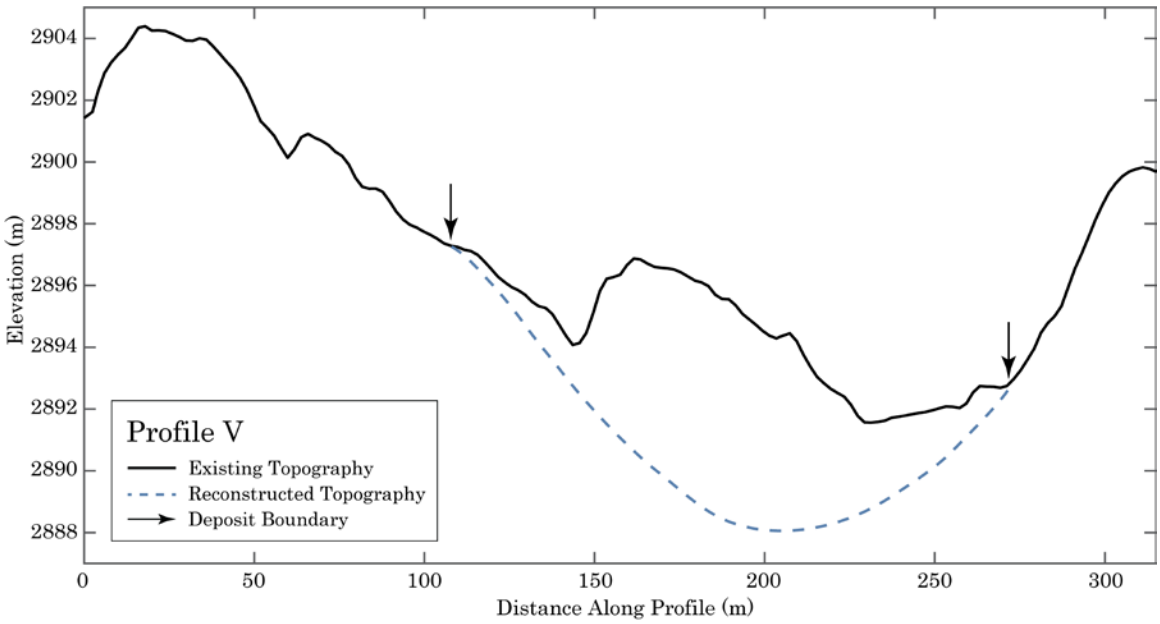

Figure 33
Profile V

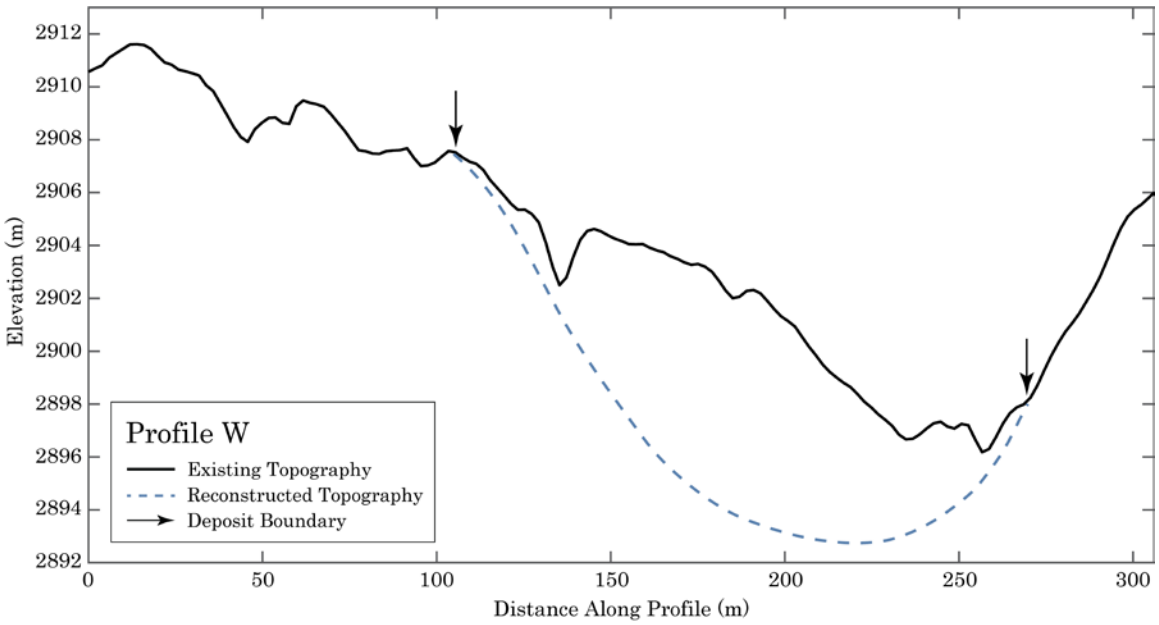

Figure 34
Profile W

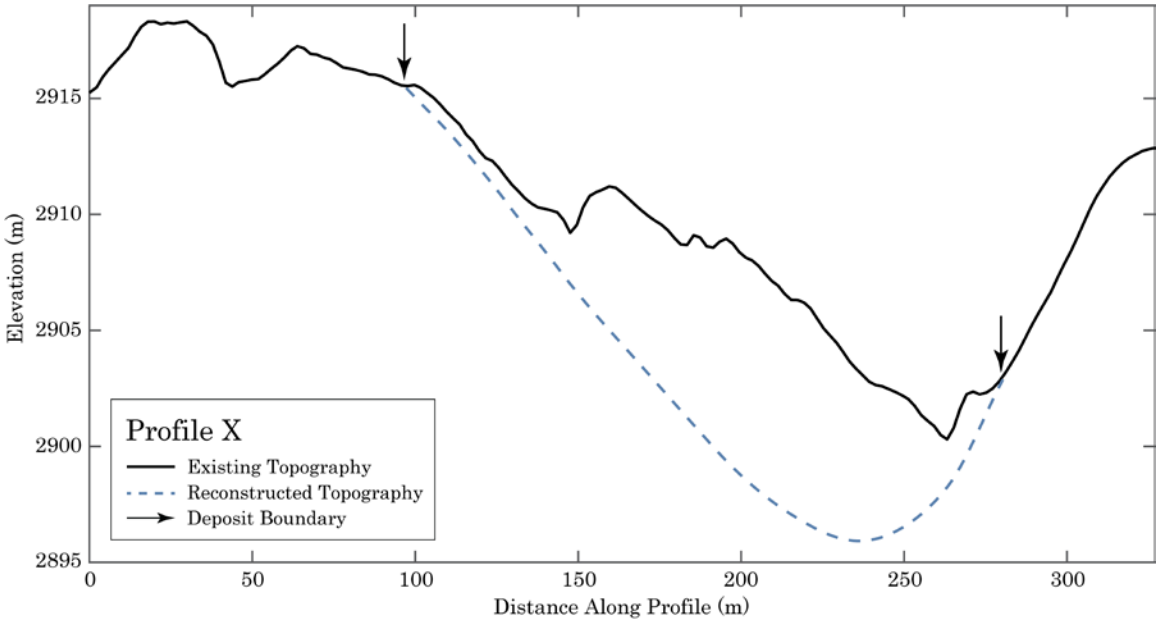

Figure 35
Profile X

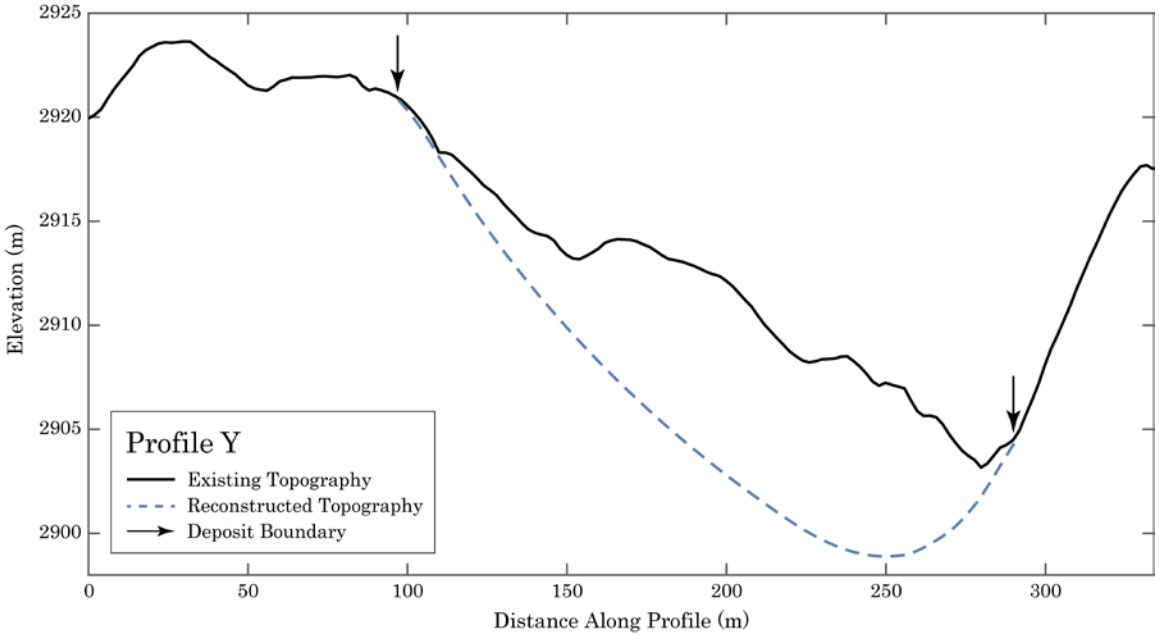

Figure 36
Profile Y

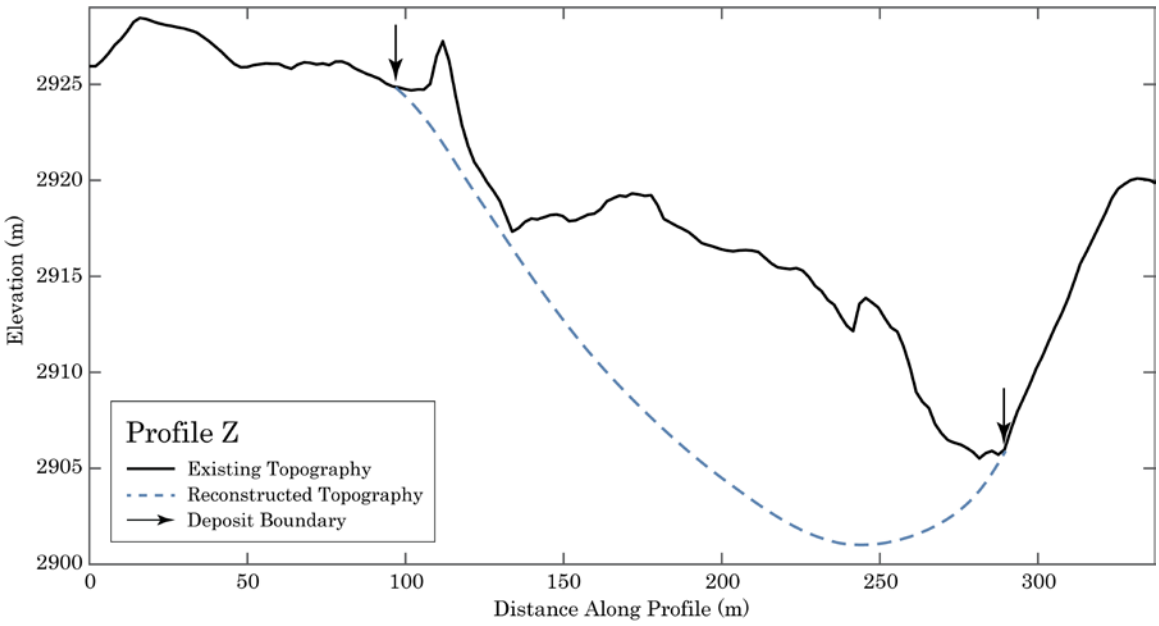

Figure 37
Profile Z

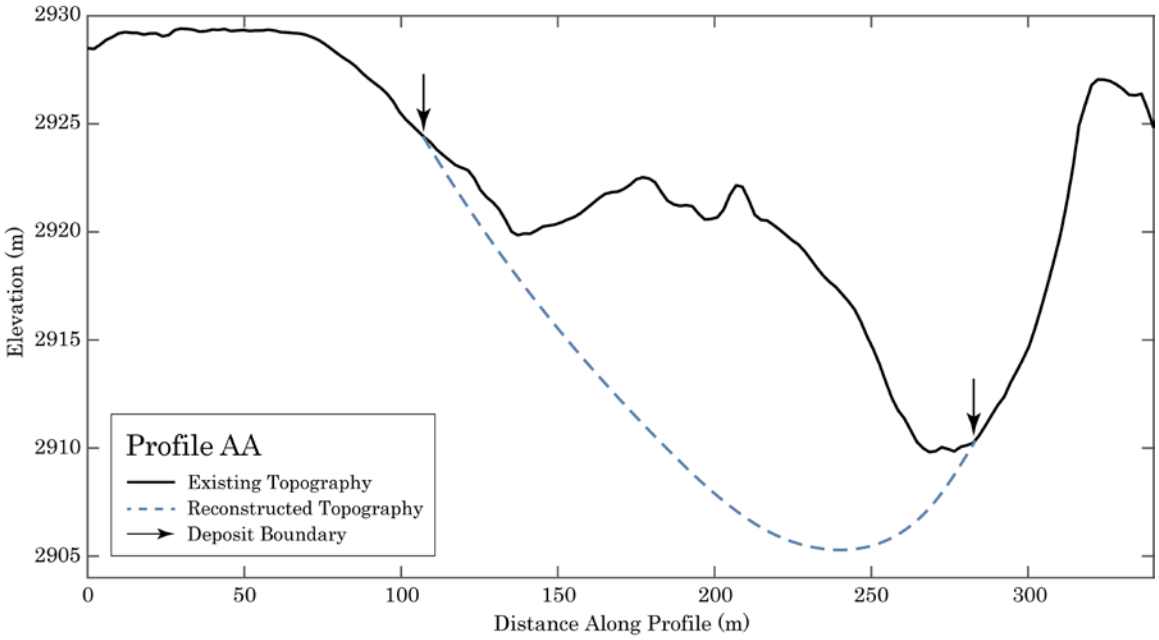

Figure 38
Profile AA

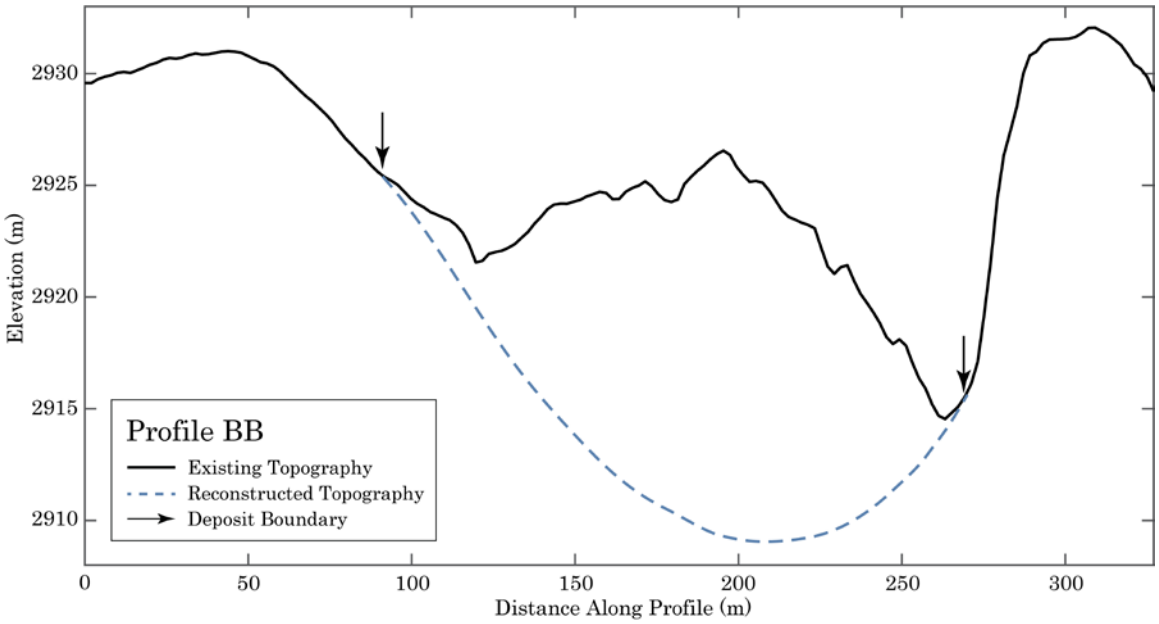

Figure 39
Profile BB

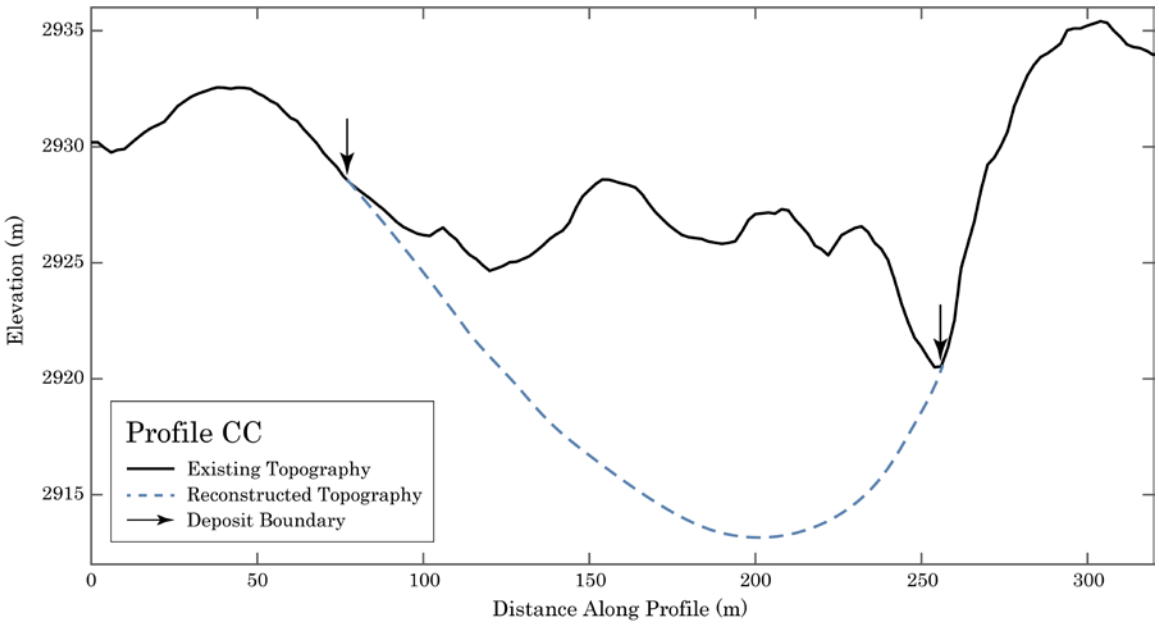

Figure 40
Profile CC

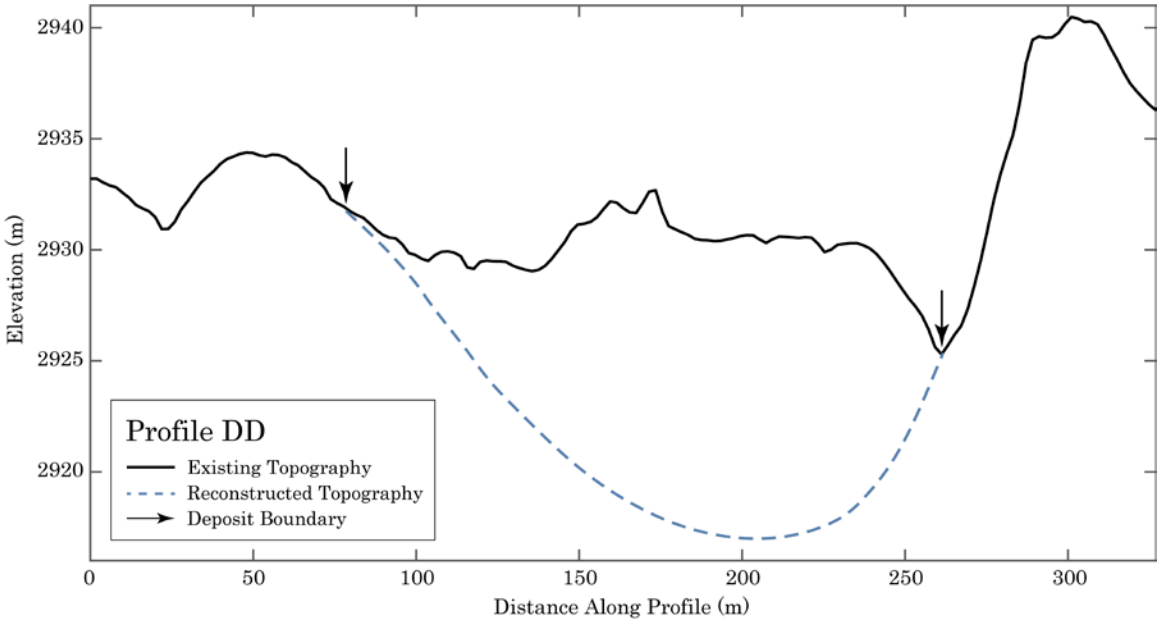

Figure 41
Profile DD

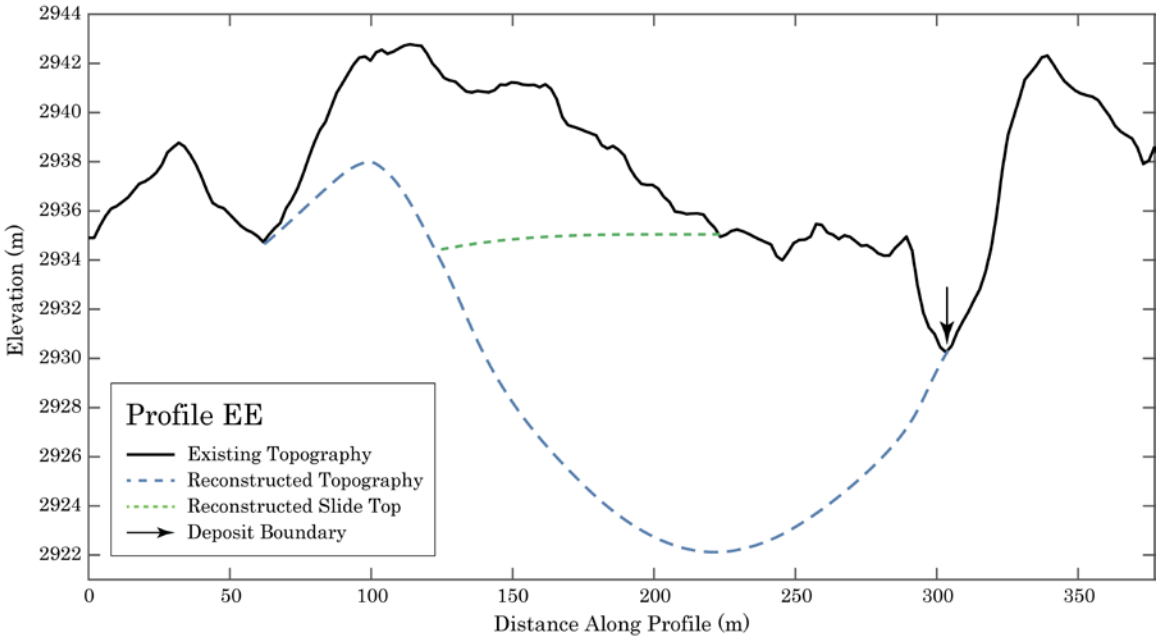

Figure 42
Profile EE

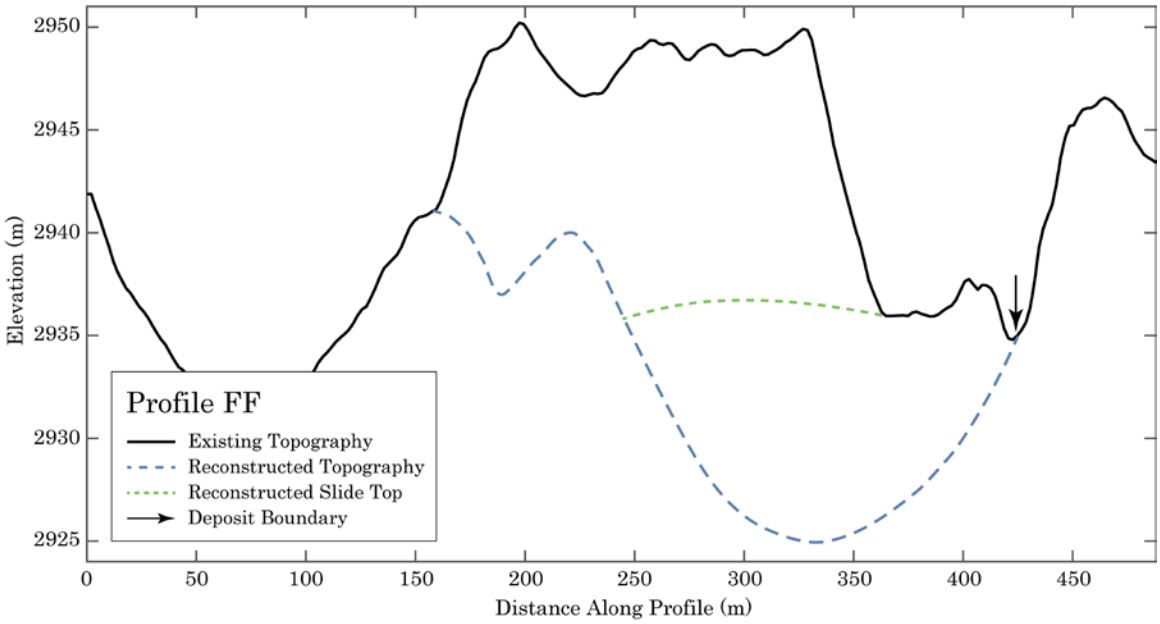

Figure 43
Profile FF

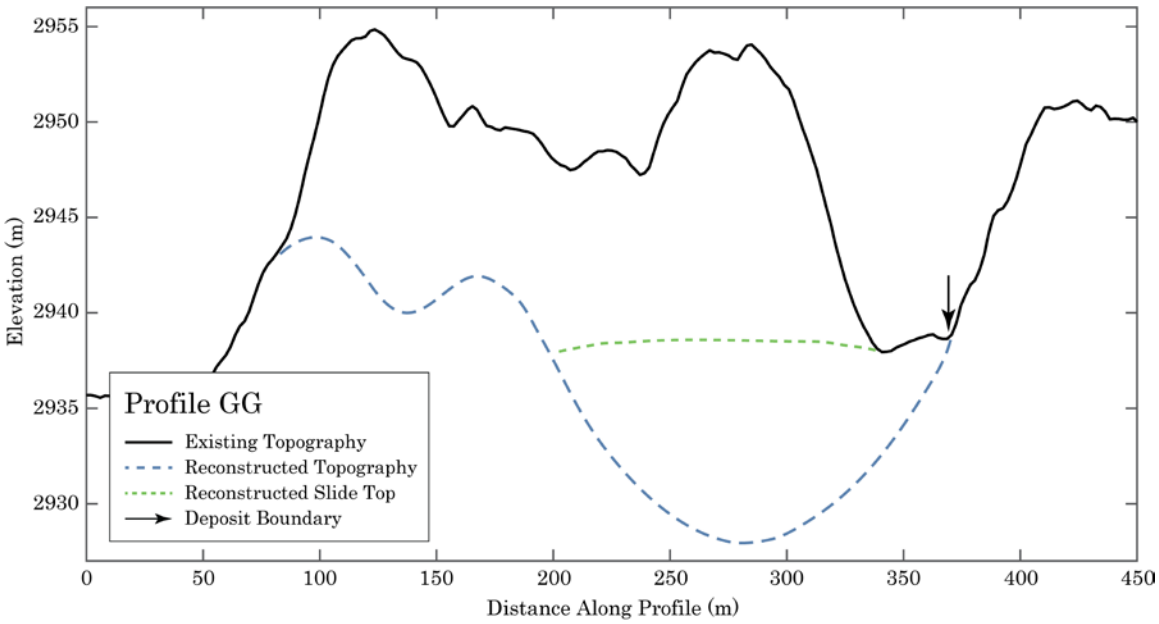

Figure 44
Profile GG

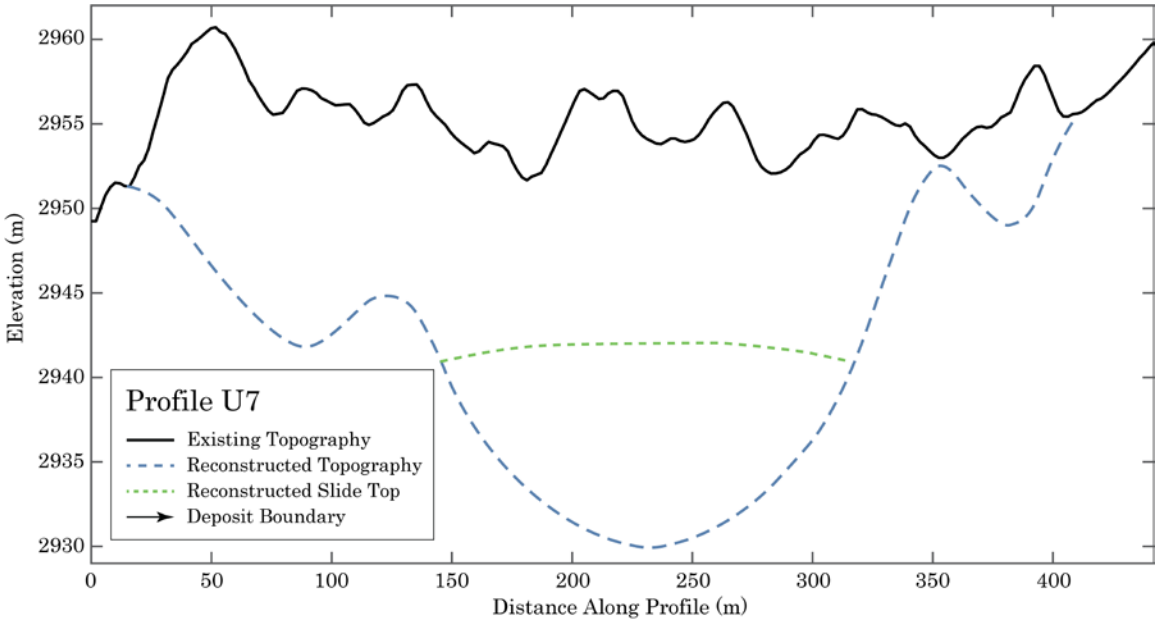

Figure 45
Profile U7

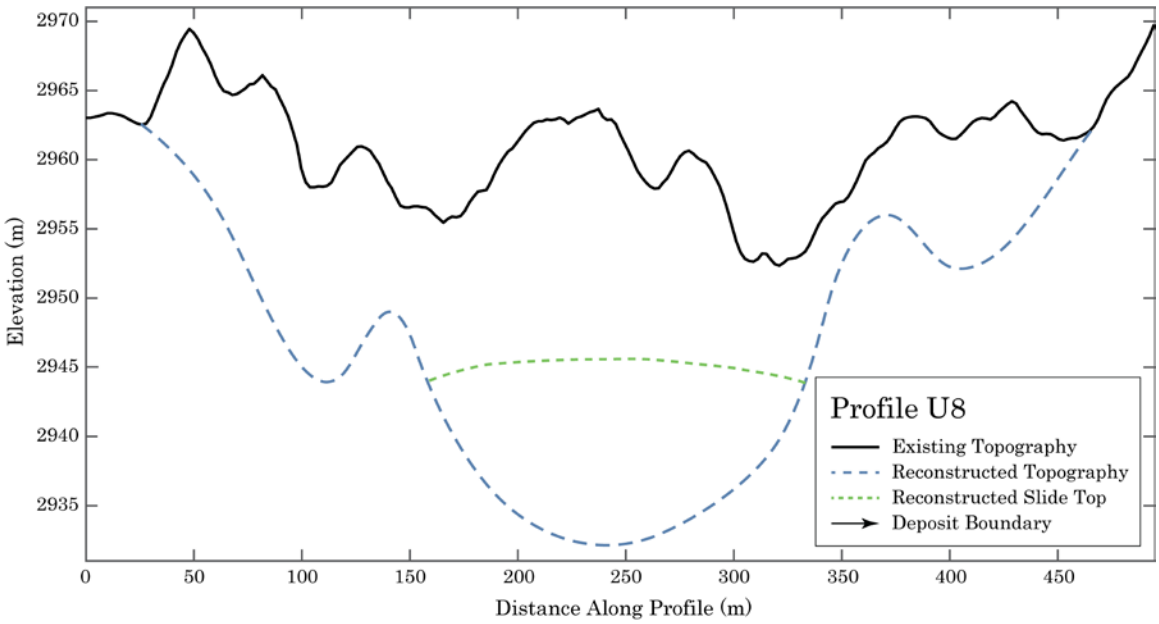

Figure 46
Profile U8

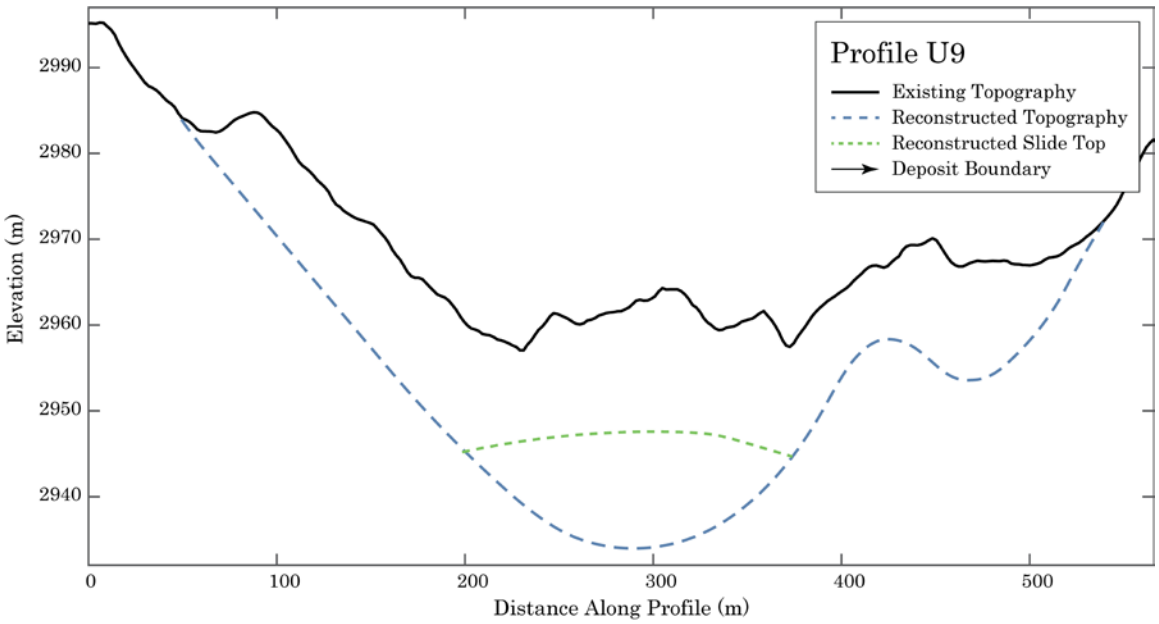

Figure 47
Profile U9

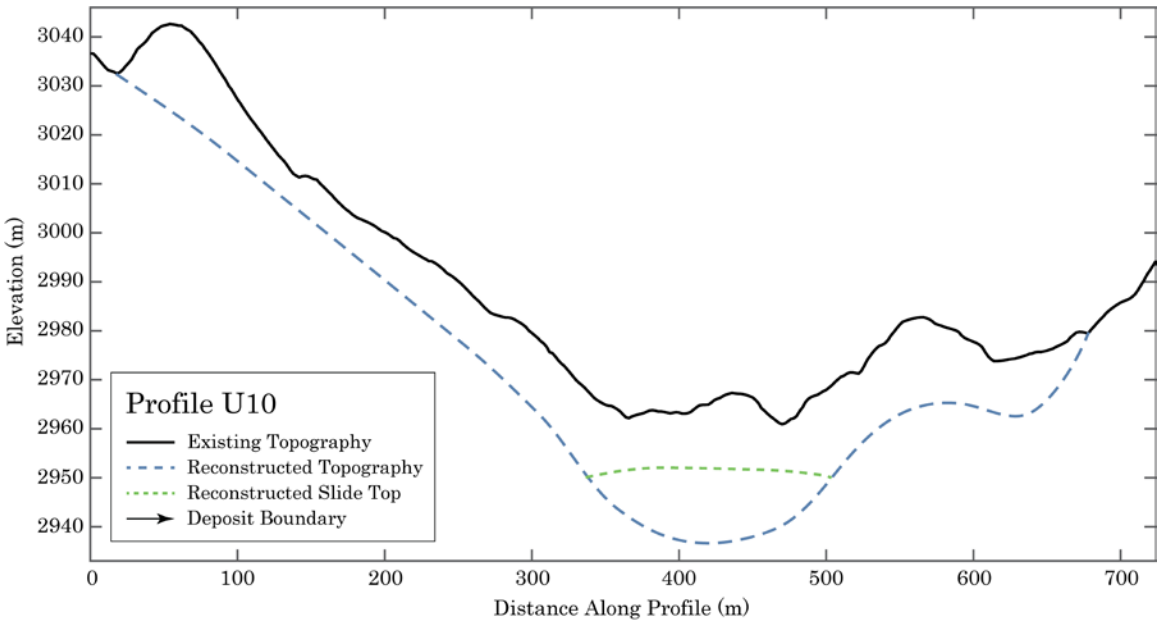

Figure 48
Profile U10

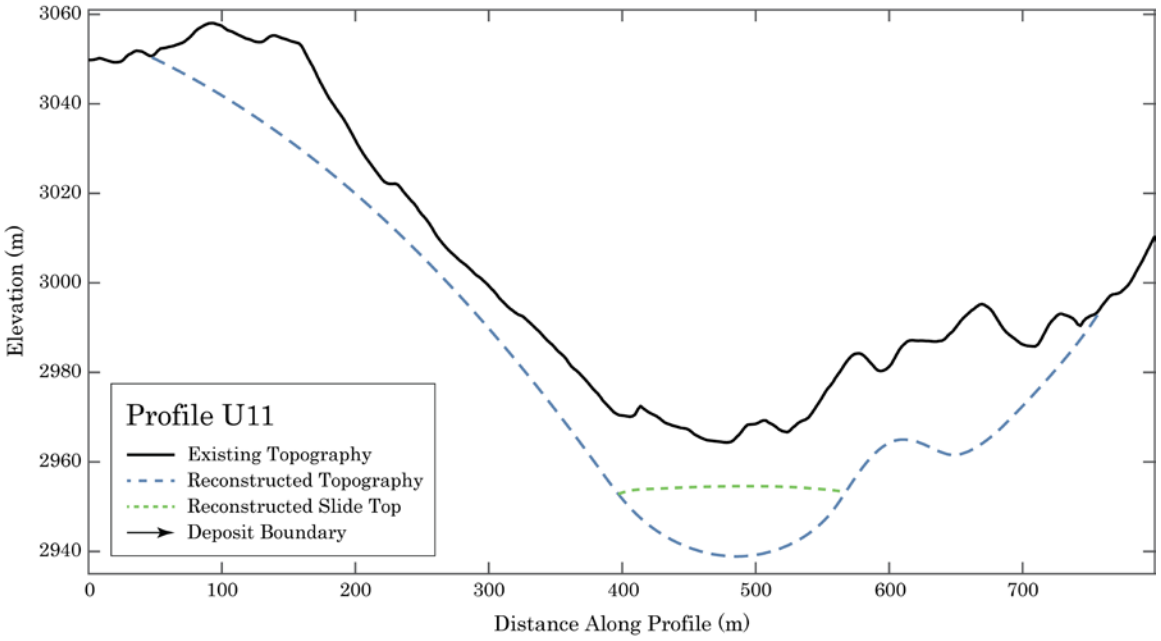

Figure 49
Profile U11

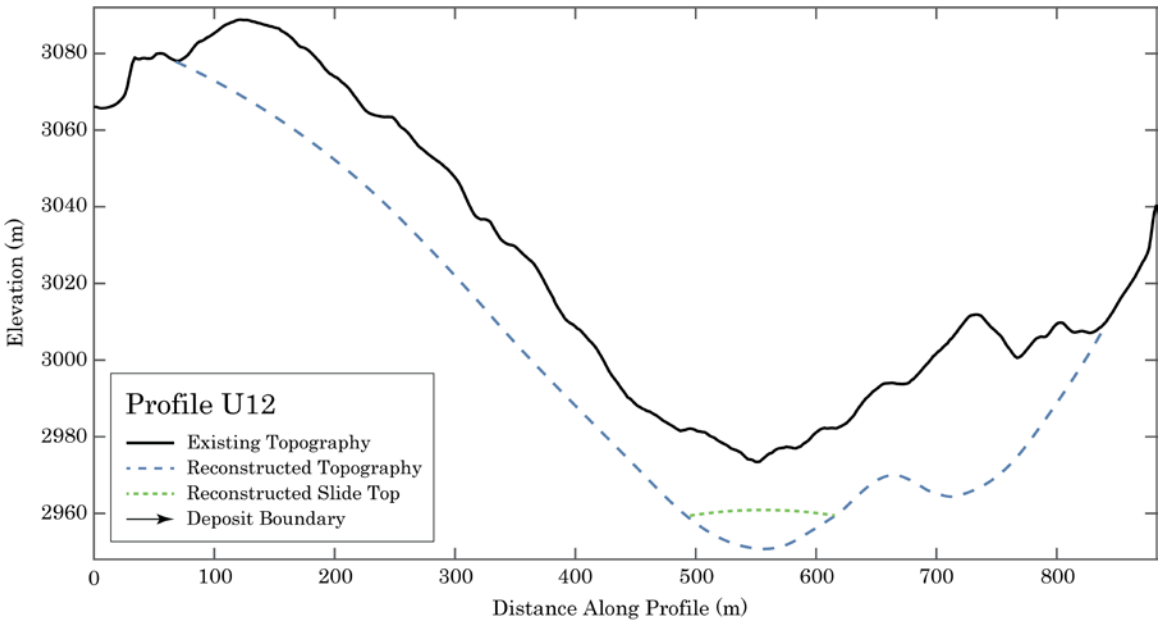

Figure 50
Profile U12

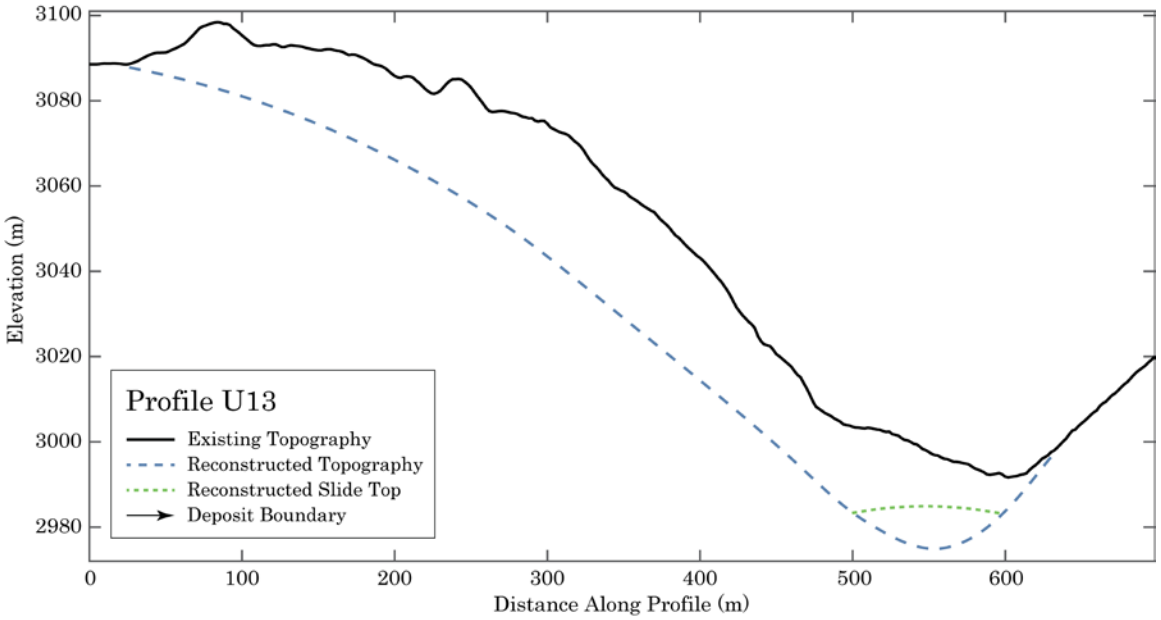

Figure 51
Profile U13

REFERENCES

Aaron, J., and O. Hungr, 2016, Dynamic analysis of an extraordinarily mobile rock avalanche in the Northwest Territories, Canada: Canadian Geotechnical Journal, v. 53, no. 6, p. 899–908, doi:10.1139/cgj-2015-0371.

Albion Basin transportation feasibility study, 2011: Salt Lake City, David Evans and Associated, Inc., Report, 159 p.

Allmendinger, R. W., 1992, Fold and thrust tectonics of the western United States exclusive of the accreted terranes, in B. C. Burchfiel, P. W. Lipman, and M. L. Zoback, eds., The Cordilleran orogen, conterminous U.S.: Boulder, Geological Society of America, p. 583–608.

Anderson, R. S., and S. P. Anderson, 2010, Geomorphology: Cambridge, Cambridge University Press, 637 p.

Ashland, F. X., and G. N. McDonald, 2008, Reconnaissance of the Grandview Peak rock slide, Salt Lake County, Utah – A possible earthquake-induced landslide?: Salt Lake City, Utah Geological Survey Open File Reports no. 518, p. 1–13.

Baker, A. A., F. C. Calkins, M. D. Crittenden, and C. S. Bromfield, 1966, Geologic map of the Brighton Quadrangle, Utah: United States Geological Survey Geologic Quadrangle Map GQ-534, scale 1:24,000, 1 sheet.

Ballantyne, C. K., J. O. Stone, and L. K. Fifield, 1998, Cosmogenic Cl-36 dating of postglacial landsliding at The Storr, Isle of Skye, Scotland: The Holocene, v. 8, p. 347–351, doi:10.1191/095968398666797200.

Cardoso, R. K., 2002, Timing and mechanics of the White Pine rockslide in Little Cottonwood Canyon, Master of Science Thesis, University of Utah, Salt Lake City, 77 p.

Case, W. F., S. N. Eldredge, M. R. Milligan, and C. Wilkerson, 2005, Geologic guide to the Central Wasatch Front Canyons: Salt Lake City, Utah Geological Survey Public Information Series 87, 18 p.

Christenson, G. E., and F. X. Ashland, 2006, Assessing the stability of landslides - Overview of lessons learned from historical landslides in Utah: 40th Symposium on Engineering Geology and Geotechnical Engineering 2006, p. 1–17.

Coe, J., R. R. L. Baum, K. E. Allstadt, B. F. Kochevar, R. G. Schmitt, M. L. Morgan, J. L. White, B. T. Stratton, T. A. Hayshi, and J. W. Kean, 2016, Rock-avalanche dynamics revealed by large-scale field mapping and seismic signals at a highly mobile avalanche in the West Salt Creek valley, western Colorado: Geosphere, v. 12, no. 2, p. 607–631, doi: https://doi.org/10.1130/GEOS01265.1

Coe, J. A., E. K. Bessette-Kirton, and M. Geertsema, 2017, Increasing rock-avalanche size and mobility in Glacier Bay National Park and Preserve, Alaska detected from 1984 to 2016 Landsat imagery: Landslides, no. February, p. 1–15, doi:10.1007/s10346-017-0879-7.

Collins, B. D., and G. M. Stock, 2016, Rockfall triggering by cyclic thermal stressing of exfoliation fractures: Nature Geoscience, v. 9, no. 5, p. 395–400, doi:10.1038/ngeo2686.

Crittenden, M. D., 1976, Stratigraphic and structural setting of the Cottonwood area, Utah: Symposium on Geology of the Corilleran Hingeline: Rocky Mountain Association of Geologists, p. 363–379.

Davidson, C., 2011, Rock avalanches, Master of Science Thesis, University of British Columbia, Vancouver, 13 p.

Deline, P., K. Hewitt, N. Reznichenko, and D. Shugar, 2014, Rock Avalanches onto Glaciers, in J. Shroder, and T. Davies, eds., Landslide Hazards, Risks, and Disasters: Amsterdam, Elsevier, p. 263–319, doi:10.1016/B978-0-12-396452-6.00009-4.

Dufresne, A., 2009, Influence of runout path material on rock and debris avalanche mobility : field evidence and analogue modelling, Doctor of Philosophy Dissertation, University of Canterbury, Christchurch, 268 p.

DuRoss, C. B., 2008, Holocene vertical displacement on the central segments of the Wasatch fault zone, Utah: Bulletin of the Seismological Society of America, v. 98, no. 6, p. 2918–2933, doi:10.1785/0120080119.

Evans, S. G., K. B. Delaney, R. L. Hermanns, A. Strom, and G. Scarascia-mugnozza, 2011, The formation and behavior of natural and artificial rockslide dams; Implications for engineering performance and hazard management, in S. G. Evans, R. L. Hermanns, A. Strom, and G. Scarascia-Mugnozza, eds., Natural and artificial rockslide dams: New York, Springer, p. 1–75, doi:10.1007/978-3-642-04764-0.

Favreau, P., A. Mangeney, A. Lucas, G. Crosta, and F. Bouchut, 2010, Numerical modeling of landquakes: Geophysical Research Letters, v. 37, no. 15, p. 1–5, doi:10.1029/2010GL043512.

Gischig, V. S., J. R. Moore, K. F. Evans, F. Amann, and S. Loew, 2011, Thermomechanical forcing of deep rock slope deformation: 1. Conceptual study of a simplified slope: Journal of Geophysical Research: Earth Surface, v. 116, no. 4, p. 1–18, doi:10.1029/2011JF002006.

Grämiger, L. M., J. R. Moore, C. Vockenhuber, J. Aaron, I. Hajdas, and S. Ivy-Ochs, 2016, Two early Holocene rock avalanches in the Bernese Alps (Rinderhorn, Switzerland): Geomorphology, v. 268, p. 207–221, doi:10.1016/j.geomorph.2016.06.008.

Grämiger, L. M., J. R. Moore, V. S. Gischig, S. Ivy-Ochs, and S. Loew, 2017, Beyond debuttressing: Mechanics of paraglacial rock slope damage during repeat glacial cycles: Journal of Geophysical Research: Earth Surface, v. 122, no. 4, p. 1004–1036, doi:10.1002/2016JF003967.

Hooper, W. G., 1951, Geology of the Smith and Morehouse-South Fork area, Utah, Master of Science Thesis, University of Utah, Salt Lake City, 60 p.

Hungr, O., and S. G. Evans, 1996, Rock avalanche runout prediction using a dynamic model: Proceedings of the 7th International Symposium on Landslides, Trondheim, Norway, v. 17, no. 1955, p. 21.

Hungr, O., and S. G. Evans, 2004, Entrainment of debris in rock avalanches: An analysis of a long run-out mechanism: Bulletin of the Geological Society of America, v. 116, no. 9–10, p. 1240–1252, doi:10.1130/B25362.1.

Hungr, O., and S. McDougall, 2009, Two numerical models for landslide dynamic analysis: Computers and Geosciences, v. 35, no. 5, p. 978–992, doi:10.1016/j.cageo.2007.12.003.

Ivy-Ochs, S., H. Kerschner, A. Reuther, F. Preusser, K. Heine, M. Maisch, K. P. W., and C. Schluchter, 2008, Chronology of the last glacial cycle in

the European Alps: Journal of Quaternary Science, v. 23, no. 6–7, p. 559–573, doi:10.1002/jqs.

Ivy-Ochs, S., and F. Kober, 2008, Surface exposure dating with cosmogenic nuclides: Quaternary Science Journal (Eiszeitalter und Gegenwart), v. 57, p. 179–209, doi:10.328.

Ivy-Ochs, S., A. v. Poschinger, H. A. Synal, and M. Maisch, 2009, Surface exposure dating of the Flims landslide, Graubünden, Switzerland: Geomorphology, v. 103, no. 1, p. 104–112, doi:10.1016/j.geomorph.2007.10.024.

Jibson, R. W., E. L. Harp, W. Schulz, and D. K. Keefer, 2006, Large rock avalanches triggered by the M 7.9 Denali Fault, Alaska, earthquake of 3 November 2002: Engineering Geology, v. 83, no. 1–3, p. 144–160, doi:10.1016/j.enggeo.2005.06.029.

Keefer, D. K.,1984, Landslides caused by earthquakes: Geological Society of America Bulletin, v. 95, p. 406–421.

Laabs, B. J. C., and J. S. Munroe, 2016, Late Pleistocene mountain glaciation in the Lake Bonneville basin, in C. G. Oviatt, ed., Lake Bonneville: A scientific update: Amsterdam, Netherlands, Elsevier, p. 462–498.

Lipovsky, P. S., et al., 2008, The July 2007 rock and ice avalanches at Mount Steele, St. Elias Mountains, Yukon, Canada: Landslides, v. 5, no. 4, p. 445–455, doi:10.1007/s10346-008-0133-4.

Loew, S., 2012, Monitoring of potentially catastrophic rockslides: 11th International & 2nd North American Symposium on Landslides, p. 101–116.

Madsen, D. B., and D. R. Currey, 1979, Late Quaternary glacial and vegetation changes: Quaternary Research, v. 12, no. 2, p. 254–270.

McCalpin, J. P., 2002, Post-Bonneville paleoearthquake chronology of the Salt Lake City segment, Wastch Fault Zone, from the 1999 "megatrench" site: Salt Lake City, Utah Geological Survey Miscellaneous Publication 02-7, 45 p.

McColl, S. T., 2012, Paraglacial rock-slope stability: Geomorphology, v. 153–154, p. 1–16, doi:10.1016/j.geomorph.2012.02.015.

McColl, S. T., T. R. H. Davies, and M. J. McSaveney, 2010, Glacier retreat and rock-slope stability: debunking debuttressing: Delegate Papers, Geologically Active, 11th Congress of the International Association for

Engineering Geology and the Environment, Auckland, Aotearoa, 5–10 September 2010. Auckland, New Zealand, p. 467–474.

McCoy, W. D., 1977, A reinterpretation of certain aspects of the glacial history, Master of Arts Thesis, University of Utah, Salt Lake City, 94 p.

McDougall, S., and O. Hungr, 2004, A model for the analysis of rapid landslide motion across three-dimensional terrain: Canadian Geotechnical Journal, v. 41, no. 6, p. 1084–1097, doi:10.1139/t04-052.

McDougall, S., M. McKinnon, and O. Hungr, 2012, Developments in landslide runout prediction, in J. J. Clague and D. Stead, eds., Landslides: Types, mechanisms and modeling: Cambridge, Cambridge University Press, p. 187–195.

Pankow, K., W. J. Arabasz, R. Carey, G. Christenson, J. Groeneveld, B. Maxfield, P. W. McDonough, B. Welliver, and T. L. Youd, 2015, Scenario for a magnitude 7.0 earthquake on the Wasatch Fault – Salt Lake City Segment: hazards and loss estimates: Salt Lake City, 57 p.

Reimer, P. J. et al., 2013, IntCal13 and Marine13 Radiocarbon Age Calibration Curves 0–50,000 Years cal BP: Radiocarbon, v. 55, no. 4, p. 1869–1887, doi:10.2458/azu_js_rc.55.16947.

Richmond, G. M., 1964, Glaciation of Little Cottonwood and Bells Canyons, Wasatch Mountains, Utah: Professional Paper 454-D, p. 1–45, doi:10.1021/nn204239d.

Robertson, R. W., 1972, This is Alta: Salt Lake City, Alta Historical Society, 80 p.

Sanders, J. W., K. M. Cuffey, J. R. Moore, K. R. MacGregor, and J. L. Kavanaugh, 2012, Periglacial weathering and headwall erosion in cirque glacier bergschrunds: Geology, v. 40, no. 9, p. 779–782, doi:10.1130/G33330.1.

Sherard, J. L., R. J. Woodward, S. F. Gizienski, and W. A. Clevenger, 1963, Earth and earth-rock dams: New York, John Wiley and Sons, Inc., 725 p.

Shrontz, D., 1989, Alta: A People's Story: Salt Lake City, University of Utah Printing Service, 142 p.

Sovilla, B., and P. Bartelt, 2002, Observations and modelling of snow avalanche entrainment: Natural Hazards and Earth System Sciences, v. 2, no. 3–4, p. 169–179, doi:10.5194/nhess-2-169-2002.

Stock, G. M., and R. A. Uhrhammer, 2010, Catastrophic rock avalanche 3600 years BP from el Capitan, Yosemite Valley, California: Earth Surface Processes and Landforms, v. 35, no. 8, p. 941–951, doi:10.1002/esp.1982.

Swan, F. H., K. L. Hanson, and D. P. Schwartz, 1980, Study of earthquake recurrence intervals on the Wasatch Fault, Utah: Salt Lake City, United States Geological Survey Open File Report no. 81-450, 55 p.

Utah Automated Geographic Reference Center, State Geographic Information Database, 2006, 2-meter LiDAR data, http://gis.utah.gov/data/elevation-terrain-data/2-meter-lidar/ (accessed September 2015)

Utah Geological Survey Aerial Imagery Collection, n.d., 1940 COH 2-8 photographed August 10, 1940, 1963 ELK 4-28 photographed June 26, 1963, https://geodata.geology.utah.gove/imagery/ (accessed June 2016)

Willenberg, H., E. Eberhardt, S. Loew, S. McDougall, and O. Hungr, 2009, Hazard assessment and runout analysis for an unstable rock slope above an industrial site in the Riviera valley, Switzerland: Landslides, v. 6, no. 2, p. 111–116, doi:10.1007/s10346-009-0146-7.

Wong, I., et al., 2016, Earthquake Probabilities for the Wasatch Front Region in Utah, Idaho, and Wyoming: Salt Lake City, Utah Geological Survey Miscellaneous Publication 16-3, 418 p.